UNIVERSITY OF TURIN

Department of Neuroscience *Rita Levi Montalcini*

PhD program in Experimental Medicine and Therapy

XXXV Cycle

DOCTORAL DISSERTATION

Sleep fragmentation accelerates Alzheimer's disease pathology in 5xFAD mouse model and affects memory consolidation in young wild-type mice through glymphatic system alteration

Thesis' author: Valeria Vasciaveo
Supervisor: Elena Tamagno
PhD program Co-ordinator: Pasquale Pagliaro

Academic years of enrolment: 2019/2023

Code of scientific discipline: General Pathology (MED04)

To my family.

Index

Introduction

Alzheimer's disease

Epidemiology

As the average lifespan continues to extend, diseases that significantly correlate with aging, such as cardiovascular diseases, cancer, arthritis, cataracts, osteoporosis, type 2 diabetes, hypertension, and dementia, have emerged as increasingly urgent concerns. Notably, people over the age of 60 were 1 billion in 2020, this age category will double to 2.1 billion people by 2050. The World Health Organization (WHO) estimates that more than 55 million people in the world are affected by dementia in 2019, which is expected to rise to 139 million by 2050, and the costs associated are expected to double from 1.3 trillion per year in 2019 to 2.8 trillion dollars by 2030[1]. The most common form of dementia (60-80% of the cases) is Alzheimer's disease (AD), with less than 50% is pure AD and the majority is expected to be mixed dementias[2]. AD is among the leading causes of death worldwide, and the rate continues to rise precisely because of the lack of decisive treatments. Aging is the strongest risk factor for AD, with the incidence for all dementias doubling every 6.3 years[1]. As the incidence of AD increases exponentially with age, this growth trend will be accompanied by a dramatic increase in the number of cases of this disease with a huge socioeconomic cost.

Etiology

AD is a progressive neurodegenerative disorder characterized by loss of both new memory acquisition and short-term memory. It is classified in two forms: sporadic or late onset, which is the most common form of AD; and the earlier onset or familiar AD. The latter is rare, only in 5% of the cases, and it is characterized by genetic mutations with high penetrance and dominant autosome transmission in three different genes: amyloid-precursor protein (APP) and the two genes of presenilin 1 and 2 (PSEN1 and PSEN2) associated to the catalytic activity of gamma-secretase[3]. The study of AD dominant autosome forms gave important information for the comprehension of disease pathogenesis, because the three genes involved are tightly linked to amyloid-β (Aβ) production, which is the main component of senile plaques. Although many genetic risk factors were studied in these years, a definitely genotype for the late onset form is not yet identified. Indeed, AD is classified more as a multifactorial disorder, in which the first risk factor is aging accompanied by cardiovascular diseases, diabetes, hypertension, obesity, and many others. Indeed, with a longer mid-life, AD is an important and present problem. It is among the first cause of death in Italy and the percentage arises just for the lack of resolutive therapies[4].

Alzheimer's disease pathogenesis

About 100 years ago, Alois Alzheimer first described the principal features of amyloid plaques and neurofibrillary tangles (NTFs), which are still necessary for the pathological diagnosis of the disease that bears his name[5]. In addition to extracellular amyloid plaques and intracellular NTFs, activated microglia and astrocytes can be detected for diagnosis. Literature data indicates that amyloid deposition and tau pathology in AD can precede structural changes in the brain, including hippocampal volume loss and decreased glucose metabolism, by decades (15-20 years before the symptoms)[6]. Since AD is mostly associated to other dementias or pathologies, the symptoms can be different in some AD subtypes. In fact, pathological findings of high probability of AD could be thought to be affected by other disorders, accentuating the fact that AD neuropathological changes are often in co-morbidity with other diseases. All these concerns allow us to consider AD as multifactorial disorder in which most of the risk factors play an important role in its pathogenesis. This highlights the difficulties in diagnosing the disease and the importance of prevention[7].

Amyloid plaques

Neuropathologically, AD is characterized by amyloid plaques, neurofibrillary tangles and neuroinflammation in the brain which lead to loss of neurons and synapses. In 1984, George Glenner and Caine Wong defined for the first time the amyloid cascade hypothesis, in which extracellular fibrillar deposits, which are constituted by amyloid-β peptides (Aβ), represent the key event in the pathogenesis of the disease[8]. Suddenly, an intense research activity was open to investigate the toxicity mechanisms of Aβ, thus leading to the discovery of new therapeutic approaches. Aβ derives from two endoproteolytic sequential cleavages made on its precursor protein APP (amyloid precursor protein): firstly, the β-secretase enzyme (BACE1) cleaves APP producing a soluble extracellular fragment and another anchored to the membrane composed of 99 amino acids (C99). This last fragment is then cleaved by γ-secretase generating Aβ peptides with different length: mainly Aβ40 and Aβ42 that is more toxic. Mutations on PSEN1 and PSEN2 genes, which express the catalytic core of γ-secretase, induce alterations in the cleavages leading to an increase in Aβ production[9,10]. Literature studies show that these mutations activate BACE1 expression, which is the other important enzyme for Aβ production[11]. The increase in BACE1 levels were also observed in the cerebral samples of sporadic AD patients[12].

Neurofibrillary tangles

In some AD post-mortem brains were observed intracytoplasmic paired-helical filaments (PHF) in several neurons located in the entorhinal cortex, limbic areas, hippocampus, and the amygdala. These PHFs are mainly formed by tau proteins[13,14]. Tau is a microtubule stabilizing protein, which physiologically undergoes different post-translational modifications. Contrary to primary tauopathies, like frontotemporal dementia, which are determined by tau gene (MAPT) mutations, in secondary tauopathies, like AD, tau protein is not mutated, but it becomes toxic because of many post-translational modifications, such as hyperphosphorylation. When hyperphosphorylated, tau is no longer able to stabilize microtubules and it begins to aggregate leading to intracellular neurofibrillary tangle (NFT) formation. The probability of aggregation lies on the amino acid sequence: tau is mostly hydrophilic, but it contains a small number of hydrophobic residues, which are of low complexity and repetitive[15].

Intracellular tau tangle formation results in not only structural destabilization and disruption of axonal transport due to the loss of microtubule binding, but also in a reduction in synapses and progressive neuronal apoptosis[16]. Neuronal damage leads to the release of neurofibrillary tangles into the extracellular space, which accumulate in specific areas such as the hippocampus, entorhinal cortex, amygdala, locus coeruleus, dorsal raphe nucleus, as well as in associative cortical and motor areas, thus inducing a neurotoxic state [15].

Besides AD, NFTs have been identified in over 20 different neurodegenerative diseases collectively termed tauopathies[17]. With the exception of AD, most of these diseases occur without amyloid deposition, and many are associated with tau mutations, suggesting that tau dysfunction and/or tangle formation contributes to the etiology of the disease.

Neuroinflammation

Neuroinflammation is a crucial event in AD pathogenesis. Microglia and astrocytes are the key players of neuroinflammation. Microglia are the major resident immune cells of CNS[18,19]. They originate from the embryonic yolk-sac as monocytes, and during development, they emigrate and become resident immune cells in the brain. The major functions of microglia are immune defense and homeostasis maintenance. As monocytes, microglia can change their morphology during the physiological and pathological conditions: simplifying, they convert from a ramified (resting) to ameboid (active) form[20]. Indeed, during physiological conditions, microglia present a deactivated phenotype, in which they release anti-inflammatory and neurotrophic factors[21]. While in pathological conditions, microglia can adopt the classical M1 and the alternative M2 phenotypes[22]. The M1 phenotype promotes the pro-inflammatory state, while the M2 produces anti-inflammatory

cytokines and tissue repair factors[23,24]. However, both microglia phenotypes are involved in neurodegenerative diseases, in fact, microglia can act as a double-edged sword[25]. M2 microglia is the primary responsible for removing and degrading Aβ deposits[26]. In AD, microglia activity is generally protective, but a persistence or uncontrolled inflammatory response may lead to neurotoxic factors release causing an amplification of the disease[27]. In addition, Aβ aggregates can activate microglia cells which acquire morphological and molecular changes, thus becoming disease-associated microglia (DAM)[28]. DAM microglia express particular chemokines, cytokines, receptors, and other specific factors, such as nitric oxide (NO) and ROS that can promote neuronal death[29]. A particular receptor, TLR4 (toll-like receptor 4), can bind to Aβ by activating microglia itself by driving the expression of downstream inflammatory response genes[30,31].

Similar to microglia, astrocytes experienced morphological and functional changes in pathological conditions, manifesting as hypertrophy and excess release of neurotoxic factors. These changes result in a state known as reactive astrocytes. In fact, reactive astrocytes exhibit heightened expression of key markers, such glial fibrillary acidic protein (GFAP) and vimentin, contributing to their hypertrophic appearance[32]. In the context of AD, both post-mortem studies and research with rodent models have revealed the presence of reactive astrocytes in close proximity to Aβ plaques. When GFAP and vimentin are depleted, the astrocytic response diminishes and results in an increased Aβ plaque load in the APP/PS1 mouse model of AD[33–35]. Like microglia, reactive astrocytes may display a protective role by surrounding Aβ plaques to reduce its toxicity[36]. However, several studies report that reactive astrocytes play a neurotoxicity role by binding Aβ through TLR receptor. This leads to the activation of pro-inflammatory genes and increase the production of neurotoxic factors, such as ROS, NO, and cytokines[37]. Dysregulated activation of astrocytes and microglia triggers aberrant inflammatory reactions that ultimately result in neuronal loss. In addition, contemporary research is focused on modulating the activation status of both microglia and astrocytes, with the aim of returning them to their normal, homeostatic state[38–41]. This approach has the potential to mitigate the harmful effects of inflammatory responses.

The glymphatic system

The glymphatic system is a recently discovered and is an important system in the brain that plays a crucial role in the clearance of waste products and the exchange of cerebrospinal fluid (CSF) throughout the brain. It was first described by researchers at the University of Rochester Medical Center in 2012[42]. The term *glymphatic* stands for glial-dependent lymphatic transport. The clearance of waste products from the brain includes the removal of substances like Aβ, tau protein, and other toxins that can contribute to neurodegenerative diseases like AD[42,43]. Proper functioning

of the glymphatic system is essential for maintaining brain health. Dysfunctional waste clearance mechanisms have been implicated in neurodegenerative diseases, including AD.

The glymphatic system relies on the circulation of CSF to facilitate waste removal. CSF is a clear, colorless fluid that surrounds the brain and spinal cord. The glymphatic system uses the flow of CSF to transport waste products away from brain cells[42]. The discovery of the glymphatic system has significantly advanced our understanding of brain function and waste clearance mechanisms.

Literature data has suggested that the glymphatic system becomes less efficient with age, which could contribute to the accumulation of Aβ in AD patients[44,45]. The relationship between the glymphatic system and AD is an area of active research, and while our understanding is still evolving, there are several important points to consider regarding their connection.

Glial cells, specifically astrocytes, are central to the functioning of the glymphatic system. Astrocytes establish pathways that allow CSF to circulate and assist in eliminating waste substances. These pathways are primarily composed of a water channel known as aquaporin-4 (AQP4)[46,47]. This channel facilitates the flow of CSF into the brain's parenchyma, where it merges with the interstitial fluid (ISF). This combined fluid then follows a directional flow, moving toward the perivascular and perineuronal regions before finally reaching the meningeal vessels and arachnoid granulations[48] (Fig. 1). In TgAPP/PS1 mice and AQP4-deficient mice, there is a notable 25-50% rise in Aβ levels compared with the model that does express AQP4[49]. There is emerging evidence that neuroinflammation, which is often present in AD, may affect glymphatic system function[49]. Chronic inflammation can disrupt the normal functioning of astrocytes and other glial cells, potentially impairing the glymphatic system's efficiency.

The glymphatic system is closely tied to sleep, and its activity is significantly influenced by sleep patterns. Indeed, the glymphatic system is more active during sleep, particularly during slow-wave sleep (SWS), which is a deep stage of non-REM (NREM) sleep. During SWS, brain cells shrink in size, creating more space for CSF to flow through the brain tissue. This enhanced flow facilitates the removal of waste products and toxins[50,51].

The already altered sleep architecture in the elderly, partly due to a decrease in the total NREM sleep duration, significantly contributes to a decline in ISF clearance in the brain, leading to a kind of stasis that predisposes to the formation of protein aggregates[42]. Issues related to sleep quality can therefore increase the incidence of neurodegenerative processes in the elderly and accelerate their progression[52]. Adequate and high-quality sleep is crucial for the optimal functioning of the glymphatic system. Disrupted sleep patterns, such as sleep fragmentation or sleep disorders, can hinder glymphatic activity[43]. Chronic sleep disturbances may impede brain ability to effectively clear waste products, potentially contributing to cognitive decline and neurological disorders[53].

There is growing evidence linking sleep disorders, such as sleep apnea and insomnia, to an increased risk of neurodegenerative diseases like AD[54–56]. This area of study holds promises for potential therapeutic interventions in AD by focusing on improving waste clearance mechanisms in the brain, which could help reduce the accumulation of toxic proteins and slow the progression of the disease.

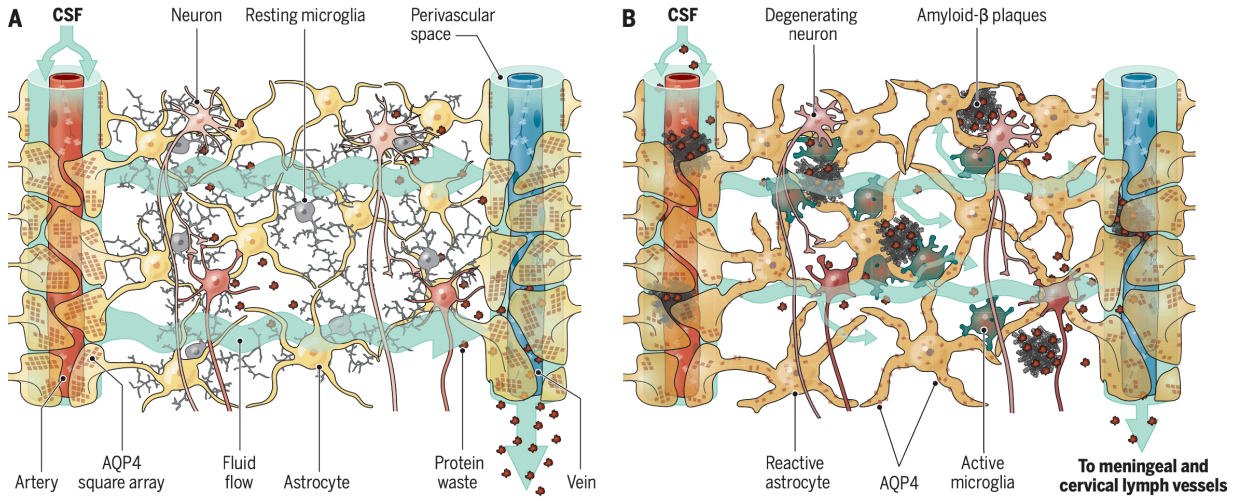

Figure 1. The brain glymphatic system in healthy and AD[48].

Sleep in healthy and disease

Sleep is a natural and essential physiological process that is crucial for overall health and well-being. It plays a vital role in various aspects of physical, mental, and emotional health. While the exact purpose of sleep is not fully understood, it is clear that sleep is essential for numerous functions: memory consolidation, cognitive function, emotional regulation, and physical recovery[57–59]. Sleep also helps the body repair tissues and maintain a strong immune system [60,61].

Sleep is not a continuous state but is organized into ordered cycles with different levels of deepness[62]. Each sleep cycle typically consists of different stages, including rapid-eye movement (REM) and non-REM (NREM) sleep. In laboratory rodents, NREM sleep is commonly referred as a single state, while in human sleep NREM architecture is further divided into stages 1 to 4. Stages 3 and 4 are the deepest stages of sleep, and are referred to collectively as SWS on the basis of the patterns of large, slow (0.5–4-Hz) oscillations observed through electroencephalography (EEG)[63] (Fig. 2).

NREM sleep is characterized by muscle relaxation, decreased body temperature, and reduced heart and respiratory rates. On the other hand, REM sleep feature is the presence of both rapid eye movements and a desynchronized EEG pattern consisting of low-voltage, high frequency

waves[64,65]. Moreover, REM sleep is also characterized by completely loss of postural muscle tone, autonomic instability with higher and variable heart and respiratory rates, and cessation of thermoregulation[64,65]. Sleep stages differ not only in sleep depth, but also in the frequency and intensity of dreaming, muscle tone, neuromodulation of cortical circuits, regional brain activation, communication between memory systems, and EEG oscillations[66]. Indeed, sleep stages can be recognized thanks to the integrated analysis of data result from EEG channels and polygraphs, particularly electromyographs (EMG)[62].

The architecture and the duration of sleep stages can vary across lifespan. In young adults, sleep duration is about 7-8 h per night and go through four to six sleep cycles of 70-120 min duration. NREM sleep is mostly predominant in the first two cycles, whereas REM sleep gradually increases across the night and is most prominent in the last two cycles[62]. Aging results in marked changes in the quantity and quality of both NREM and REM sleep. Indeed, SWS stage decreases with age, while REM sleep remains quite unchanged throughout adult life[67]. These changes across lifespan are shown in several animal models, such as rodents. In fact, aging in animals is associated with sleep fragmentation, reduced sleep-wake rhythms, and altered EEG spectral profile[68–71]. Importantly, it is not just the quantity of sleep that matters but also the quality. Restorative sleep is characterized by deep, uninterrupted sleep cycles. Factors such as sleep disorders, stress, and poor sleep hygiene can disrupt sleep quality. The sleep-wake cycle is regulated by the body's internal clock, known as the circadian rhythm[72]. This rhythm helps synchronize sleep patterns with the natural light-dark cycle of the day. Exposure to natural light during the day and darkness at night helps maintaining a healthy circadian rhythm.

Various sleep disorders can disrupt normal sleep patterns resulting in a fragmented sleep. Sleep fragmentation (SF) refers to a disruption of normal sleep patterns characterized by frequent awakenings or interruptions during the night[73]. These include sleep apnea (breathing interruptions during sleep), narcolepsy (excessive daytime sleepiness), and parasomnias (unusual behaviors during sleep, like sleepwalking)[74,75]. Chronic sleep deprivation or poor-quality sleep can have significant negative effects on physical and mental health. It can lead to daytime fatigue, impaired cognitive function, mood disturbances, and an increased risk of chronic conditions such as obesity, diabetes, cardiovascular diseases, and neurodegenerative disorders[76–81]. SF can become more common with age. Indeed, older adults often experience more frequent awakenings during the night, which can contribute to sleep disturbances[82]. However, addressing underlying sleep disorders and maintaining healthy sleep habits remains important for quality sleep as individuals age. Identifying and addressing the underlying causes of SF is essential for improving sleep and well-being.

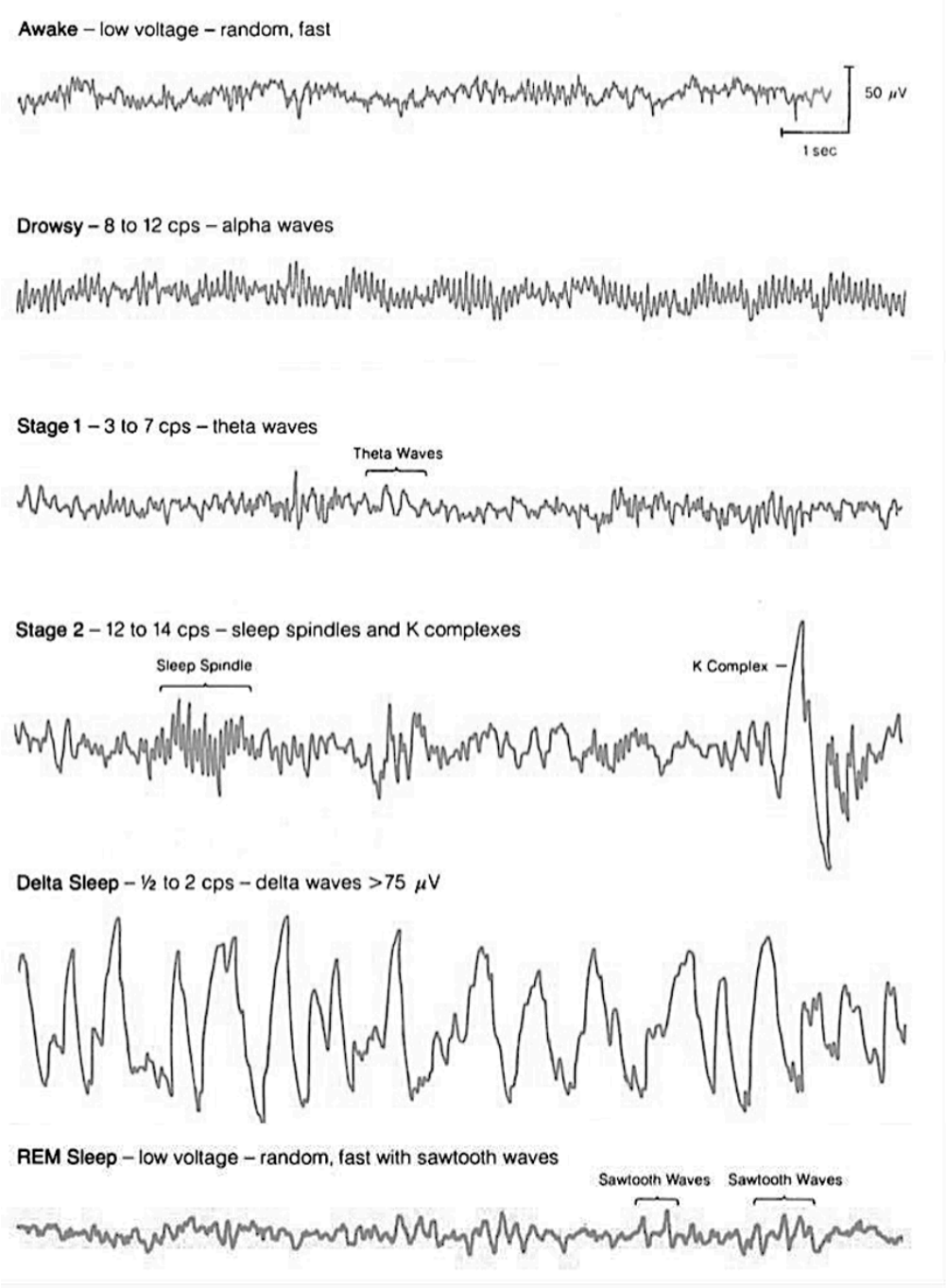

Figure 2. EEG in sleep states[163].

Sleep and memory

Memories are mostly divided into declarative and non-declarative memories. The first ones are those type of memories that a person can call to mind (e.g., the capital of Italy), the latter are memories normally used without be aware of recollection (e.g., how to ride a bicycle). Declarative memories are further divided into episodic memories, which are memories of specific events, and

semantic memories that are of general information. In the non-declarative memories, we can find procedural skills and other subcategories (Fig. 3)[83]. Currently, we know that memories are *encoded*, temporally stored, and then retrieved during wakefulness, but are consolidated and long-term stored mainly during sleep. Indeed, several data support the hypothesis that sleep stages play an important role in memory consolidation[84]. Particularly, REM sleep seems to promote procedural memories, while hippocampus-dependent declarative memories may require NREM sleep[85]. Literature data show that memory consolidation occurs firstly during NREM sleep[86]. New memories are initially stored in the hippocampus and neocortex, but they are recalled by the hippocampus. During sleep, memory consolidation occurs throughout a process in which memory sequences are repeatedly replayed. This process helps to strengthen memories in cortical areas for long-term storage and reduces the recall-dependency from the hippocampus[57]. In particular, specific wave oscillations are crucial for memory consolidation and synaptic modulation during NREM sleep. These wave oscillations are a result of neural activity that occurs between different brain regions: slow oscillations (SO) arise from several shifts in cortical neural activity alternating between an *up-state* and a *down-state*[87]; sleep spindles are coupled with SO *up-state* and originate from reticular thalamic nucleus neurons and spread to cortical and subcortical regions[88–90]; sharp-wave ripples are generated by hippocampal neurons and take place during excitable spindles[90]. This process may facilitate information flow from hippocampus to cortex and vice versa[91,92].

However, both NREM and REM sleep may be required for memory consolidation, since their amount increases after learning a new task[93,94]. Moreover, since during REM sleep most of vivid dreams occur and the EEG patterns look like similar to those of wakefulness, REM sleep seems to be a phase in which the brain recover from NREM episodes without actually waking up[95]. Some recent data suggest that NREM sleep may strengthen new memory synapses, while the pruning of those newly formed synapses occurs during REM sleep to improve the signal-to-noise ratio[96–99]. Growing evidence indicates that REM sleep might be essential for emotional memories[58,59]. In fact, selective REM sleep deprivation reduced the connectivity between the prefrontal cortex and the amygdala, which is the brain area involved in emotional processing[100].

All these data indicate that the contribution of sleep in memory consolidation is of primary importance. The consequence of sleep loss can impact cognitive functions[101,102]. With age, sleep amounts and quality decrease and this can be considered as one of the key factors for cognitive decline and neurodegenerative processes. Hence, sleep restoration may be fundamental to promote healthy aging.

In contrast to extensive research on the effects of sleep on cognition in adults, there is a relative scarcity of studies focusing on adolescents[103]. Investigating the relationship between sleep and

cognitive functions in adolescents is particularly important due to significant changes in their sleep patterns during this developmental period. Adolescence is marked by a decrease in total sleep time and a reduction in SWS[104]. This may be attributed to various factors like media exposure, late-night activities, and even school avoidance[105,106]. Understanding the impact of sleep on adolescent cognition is vital given the crucial role this developmental stage plays in learning and memory.

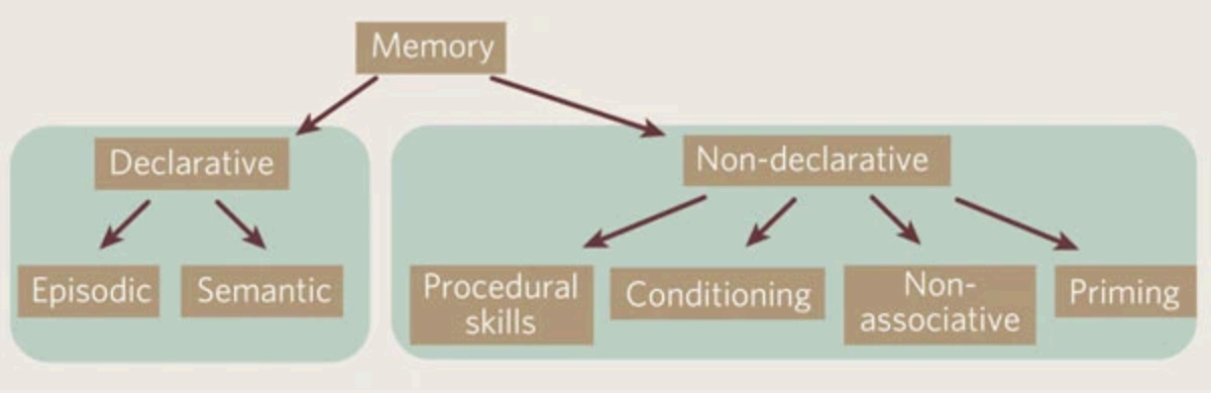

Figure 3. Memory system category.[83]

Sleep and Alzheimer's disease

Sleep disturbances are commonly associated with AD, and there is a bidirectional relationship between sleep problems and the progression of the disease. With aging, it is normal to witness a process of progressive SF and increased instability. These events are associated with a decrease in the quality and quantity of SWS, increased latency to REM sleep, a decrease in total NREM sleep, as well as a reduction in total sleep time and an increase in wake intrusions[107]. Changes in sleep architecture are often heightened in patients with mild cognitive impairment (MCI), which frequently represents a prodromal phase of AD and related dementia[108]. Sleep disturbances, including changes in sleep patterns, insomnia, and excessive daytime sleepiness, can be early signs of AD. These sleep changes may precede cognitive symptoms by several years. Poor sleep quality and sleep disruptions can adversely affect cognitive function, making it more challenging for individuals with AD to think clearly and remember things. This can exacerbate the cognitive decline associated with the disease[108]. Literature data suggests that disrupted sleep may contribute to the buildup of Aβ, as the glymphatic system is more active during deep sleep stages like NREM sleep, as mentioned above. Extracellular levels of Aβ in the ISF and CSF are higher during wakefulness and lower at night, following a 24-hour fluctuation[52]. Acute sleep deprivation increases soluble Aβ levels in the CSF by 25-30% compared to normal sleeping controls[109]. In fact,

even in very young individuals, just one night of deprivation is sufficient to cause an increase in the concentration of Aβ42 in the CSF[110]. In transgenic mice for APP and PS1, chronic sleep deprivation accelerates the deposition of Aβ; on the other hand, Aβ deposition contributes to the disruption of the sleep-wake cycle, thus resulting in an increase in total wake time[111]. Like Aβ, tau levels in the CSF decrease during the night compared with the day, and its accumulation appears to undergo a significant increase following acute sleep deprivation[112].

Managing sleep disturbances in individuals with AD can be challenging. Medications used to treat sleep problems, such as sedatives or hypnotics, may have adverse effects in older adults and those with cognitive impairment. Non-pharmacological interventions and improving sleep hygiene are often preferred approaches. Sleep disturbances in individuals with AD can also impact their caregivers. Caregivers may experience sleep disruption themselves due to the need to provide nighttime care or monitoring for their loved ones[113].

Many follow-up studies have shown that even cognitively normal individuals with high levels of SF have a 1.5 times higher risk of developing AD[114].

Strategies to enhance sleep hygiene and address sleep disorders are being explored as ways to potentially slow the progression of the disease and improve overall quality of life. Managing sleep problems is an important aspect of AD care, and ongoing research is shedding light on the complex relationship between sleep and the disease.

Aim of the study

Recently, sleep has gained growing acknowledgment as a potential marker for dementia like AD. Managing sleep problems is an important aspect of AD care, and ongoing research is shedding light on the complex relationship between sleep and the disease. The central aim of this work was to develop a new model of SF that resembles more correctly a real condition of intermittent awakening, proper of several sleep, psychiatric, and neurological disorders. This SF protocol allowed us to study the effects of sleep disorders in both the potential contribution and progression of AD. Demonstrating how nighttime intermittent arousal can worsen AD pathology can enhance our understanding of neurodegenerative processes of the disease. Additionally, studying wild-type animals helps to better comprehend how to prevent the disease.

Methods

Animals

Two-months-old no carrier male mice (control mice) and two- and six-month-old male B6SJL-Tg(APPSwFlLon, PSEN1∗M146L∗L286V)6799Vas/Mmjax (5xFAD) mice were used for a SF protocol. Experimental procedures involving the use of live animals have been carried out by the guidelines established by the European Community Directive 86/609/EEC (November 24, 1986), Italian Ministry of Health and the University of Turin institutional guidelines on animal welfare (law 116/92 on Care and Protection of living animals undergoing experimental or other scientific procedures; authorization number: 470/2021-PR). Moreover, the Ethical Committee of the University of Turin approved this type of study. The animals were maintained under 12-h light/dark cycles and were provided with water and food ‘‘*ad libitum*’’ (standard mouse chow 4RF25-GLP, Mucedola srl, Settimo Milanese, Italy). Specifically, all the procedures were carried out in order to minimize the pain and distress in the animals and we used the fewest number of animals required to obtain statistically significant data.

Sleep fragmentation protocol

Two-month-old wild type (wt) (total mice=22) and 5xFAD mice (total mice=22) and six-month-old 5xFAD mice (total mice=8) were positioned on a time-controlled tilting platforms (Stuart Scientific Platform Rocker STR6) connected to a time relay (Mini Asymmetrical Cycle Timer, AC / DC 12-240V GRT8-S2, Regun) able to regulate their activation according to a pattern of 3 minutes OFF/10 seconds ON. The mice were divided into two groups: the first group (n=11 for two-months old and n=4 for six-months old mice) underwent SF for 30 days all day long (24 h), while the second one (n=11 for two-months old and n=4 for six-months old mice) was kept in cages under the same environmental conditions as fragmented mice, but in the absence of a time-controlled tilting platform, for the same length of time. In order to evaluate the effect of the protocol on sleep-wake cycle, an electroencephalography (EEG) and electromyographic (EMG) recording was performed on three animals per group (wild type n=3 and 5xFAD n=3) for 8 days (4 days in normal sleep conditions and 4 during SF). Only the EEG data from the last day were considered, as we preferred the day when the mouse was most likely to show adaptation to the chosen fragmentation system. Each recording was analyzed considering the 24-hour day on the basis of the light/dark cycles imposed by the enclosure (8.00 am - 8.00 pm).

Surgery for EEG registration

The electrodes used for recording the electroencephalographic signal were prepared by assembling an insulated ultra-thin stainless-steel wire (0.3 mm diameter, A-M Systems, Inc.) with a stainless-steel miniature screw (diameter 1.2 mm, P1 Technologies), soldered to a connector for the electronic circuitry. The recording electrodes were put in contact with the dura mater in order to obtain an ipsilateral fronto-parietal EEG signal (referential derivation). The frontal screws (one intended to recording and one to anchor the system) were positioned +/- 1,2 mm from the interhemispheric fissure and + 1.2 from Bregma. The parietal screws (one recording and one used as common reference) were placed +/- 1.2 mm from the interhemispheric fissure and + 1.2 from Lambda. A pair of insulated ultra-thin stainless-steel wire (0.3 mm diameter, A-M Systems, Inc.) was inserted in the posterior nuchal muscle to record the electromyographic (EMG) signal [115]. During the entire procedure of implantation of the electrodes for EEG and EMG recording, the animal was deeply anesthetized with 3% isoflurane (gaseous anesthetic for veterinary use), mixed with O_2 (2 L/min) and N_2O (1 L/min), and kept on a heated support to avoid hypothermia. The whole device was firmly attached to the skull by covering it with dental cement. At the end of the surgical procedure a subcutaneous dose of ketoprofen 10 mg/kg was administered. The mice underwent the SF protocol 10 days after surgery, in order to allow adequate recovery time and post-surgery adaptation.

Acquisition of bioelectrical signals

To allow the mouse to have the greatest possible degree of freedom of movement, a structure has been developed consisting of a tilting arm capable of keeping the signal transmission cables suspended and allowing them to rotate, in such a way as to support the mouse in its movements. The EEG and EMG signals were transmitted with a cable connected to a rotating swivel commutator (SL2 + 3C/SB, P1 Technologies), used as an interface with the system responsible for the pre-amplification, amplification and A/D conversion of the signal (Grass Telefactor Comet AS40 Amplifier System for polysomnographic studies). The EEG and EMG were filtered (EEG: 0.3-35 Hz; EMG 10-70Hz; Notch filter to discard the activity in the 50Hz band) and sampled at 200Hz for data storage.

EEG data analysis

The signals acquired were manually analyzed using the Embla RemLogic-E software. The traces of the EEG and EMG data, displayed simultaneously on a 20-second time window, have been divided into mini-epochs lasting 4 seconds, and each of them has been assigned value labels: “W” for the waking epochs, “TNREM” for Non-rapid-eye-movement sleep and “TREM” for Rapid-

eye-movement sleep. Wakefulness was scored when the EMG tone was high and EEG was at low amplitude with δ and θ frequency components; NREM epochs were scored when the EMG was lower than in W and EEG was at high voltage with prominent δ frequency components; REM epochs were characterized by muscle atonia at EMG and low voltage at the EEG with predominant θ frequency components [115]. In order to assign the relative value to an epoch, the epoch must be entirely occupied by the relative stage. In cases where two different stages coexist in an epoch, it is excluded from the analysis by the label "Not scored". The total sleep time (TST) was defined as the sum of the time spent in NREM and in REM sleep.

Elevated Plus Maze (EPM)

The EPM test was used to assess anxiety-like behavior. The EPM consisted of two parallel open arms (30×5 cm, surrounded by a 0.25 cm high border) and two parallel closed arms (30×5 cm, surrounded by 15 cm high walls). The four arms join to a central platform (5×5 cm). The apparatus was raised 45 cm above the floor and was illuminated by a soft light placed in a corner of the room. The mice were placed in the room test completely in the dark or with soft light 1 h before the beginning of the test. The test was initiated by placing the mouse (n=11 per condition) on the central platform of the maze, facing one of the open arms, and leaving it free to move for 10 minutes. The behavior of the mouse was continuously recorded by a video camera placed above the apparatus, and then through the use of Ethovision XT software, the first 5 minutes were analyzed. The parameters analyzed during the test were: the frequency in open and closed arms (frequency entering in open and closed arms), the latency to enter in open arms (seconds employee to enter in open arms (sec)), the cumulative duration in closed and open arms (time spent in the different arms (sec)), the distance in the area (total distance traveled in the area (cm)), the velocity in the arena (maximum speed achieved in the area (cm/s)), the distance in the open and closed arms (distance in the different arms (cm)), and the velocity in the open and closed arms (maximum speed achieved in the different arms (cm/s) [116].

Open Field Test (OF)

The open field test (OF) was used to assess the anxiety behavior and spontaneous motor activity. The OF consisted of a square arena (60×60 cm) with a dark floor divided into 36 squares (10×10 cm). The 20 squares near the walls of the apparatus constituted the peripheral zone of the apparatus (edge) and represented the protected zone of the field, while the central 16 squares represented the exposed zone of the field or the center of the arena. The mice were placed in the test room completely in the dark or dimly lit 1 hour before the start of the test. The test began with the animal (n=11 per condition) placed in a corner of the arena and allowed to move freely for 10 min. Animal

behavior was recorded with a camera placed above the arena, and the first 5 minutes were analyzed with Ethovision XT software. The parameters analyzed during the test were the frequency of entry at the center and edges of the arena, cumulative duration at the center and edges of the arena (time spent at the center and edges of the arena (sec)), distance in the arena (total distance traveled in the arena (cm)), speed in the arena (maximum speed achieved in the arena (cm/s)), distance at the center and edges of the arena (cm), and speed at the center and edges of the arena (maximum speed achieved at the center and edges of the arena (cm/s)), the frequency of protect and un-protect rearing, and the frequency of grooming [116].

Novel Object Recognition (NOR) test

The mice were subjected to the NOR test to assess object recognition and short-term working memory [16]. The mice were placed in the test room completely in the dark or with dim light 1 hour before the start of the test. The apparatus consisted of a small opaque Plexiglas chamber with the following dimensions: 50 cm × 25 cm × 25 cm. Mice (n=11 per condition) were acclimated to the apparatus for 5 min before starting the task. The training session consisted of placing a mouse in the apparatus containing two similar objects and letting it explore for 10 minutes. The test session was performed after 60 minutes (short-term memory) in the same apparatus, but with the presence of two objects different in shape, one *familiar* and one *novel*, which the animals were allowed to explore for 5 minutes. Both phases of the test were performed in the dark, and behaviors were recorded with an infrared camera placed over the apparatus. Behavioral parameters were analyzed using Ethovision XT software and are as follows: the frequency of entry into the new and old object zones; the cumulative duration in the new and old zones, i.e., the total time spent in the different zones (sec); the frequency of interaction with the new and old objects, i.e., the frequency of times the animal sniffs the objects; the frequency of protect and un-protect rearing; and the frequency and the cumulative durations of grooming (sec). We considered also the Discrimination Index (DI), meaning the time spent exploring the novel object relative to the total time spent exploring both objects [$(N_{new} – N_{old})/(N_{new} + N_{old})$, where N_{new} represents the frequency of the interaction with the new object, while N_{old} with the old one]. The resulting score ranges from -1 to +1, when positive, the animal interacts more with the novel object, when negative with the old one. The interaction with the new object can also be expressed as a function of the Recognition Index (RI), which is the ratio of the amount of frequency exploring new objects over the total frequency exploring both objects [$N_{new}/(N_{new} + N_{old})$] [117].

Y-maze test

The y-maze test was performed to measure spatial memory. The test took place in a Y-shaped maze formed by black polyvinyl chloride panels and with three arms at an angle of 120° from each other. Mice were placed in the test room completely in the dark or dim light 1 hour before the test began. The animal (n=11 per condition) was placed in the center of the Arm 1 and allowed to freely explore the three arms. During multiple arm entries, the subject should show a tendency to enter the least recently visited arm. The number of arm entries and the number of triads are recorded to calculate the percentage of alternation. An entry occurs when all four limbs are within the arm. For the adaptation phase, mice were placed for 5 min in the maze and allowed to freely explore it. After 1 hour of rest, to evaluate the short-term memory, we tested the mice's spatial memory with all arms open and exploration of the new arm (Arm 3), for 10 min. For each session, we measured several parameters in order to assess the spatial memory, anxiety, and exploratory behaviors of the tested mice: the total distance traveled (distance traveled in the arena (cm)), the time spent in different arms (sec), the frequency of entry in different arms, the latency to enter in the new arm (sec), the frequency of protect rearing, the frequency of un-protect rearing, the frequency of grooming (n, the alternations (it is counted if the mouse enters all selected zones consecutively without repeated zone visits), the max alternations (it the total number of possible zone alternations and is calculated by taking the total number of visits and subtracting the number of selected zone minus, Alternation index=alternations/max alternations *100), and the arm entries (i.e. the order in which the mouse enters in the numbered arms) [116].

Light-dark (LD) transition test

Another test for assessing animal anxiety and, more specifically, the tendency to seek refuge in places less exposed to danger (e.g., a dark area) is the light-dark transition test. The maze consisted of two rooms with a gate between the two: one exposed to bright light and the other completely in the dark. The animal (n=6-9 per condition) was placed in the light zone and the duration of the test was about 10 minutes. The parameters analyzed during the test were: the frequency of entry into the light and dark zones, the cumulative duration in the two zones (time spent in the light and dark zones (sec)), the total distance traveled in the light zone (cm), the speed in the light zone (maximum speed achieved in the light zone (cm/s)), and the frequency of protect and un-protect rearing, and the frequency of grooming in the light zone[118].

Puzzle box (PB) test

The puzzle box maze test was the same as the light-dark transition test. In this behavioral paradigm, we analyzed working memory and problem-solving ability. To asses memory consolidation, the

test was performed in two consecutive days: in day 1 animals were trained, while they were tested in day 2. To determine memory consolidation, animals' behavior was analyzed the day after their training trails (day 2). This type of test consisted of four consecutive increasingly complicated trials. In each phase, the animal (n=6-9 per condition) was placed in a corner of the light zone and allowed to explore freely for 5 minutes. In the first training trial, we evaluated the time it took the animal to pass through the door dividing the two zones and reach the dark zone. In the second training trial, the animal had to cross a narrow underpass located under the barrier between the two zones. In the third training trial, the most difficult one, the mouse had to dig through the narrow underpass that was covered with sawdust. In day 2, the animal performed the test, which was similar to the third training trial. In this behavioral paradigm, the parameters analyzed were: the latency and frequency of entry into the dark zone; the elapsed time and frequency of digging near the narrow underpass and in the periphery of the maze; the frequency of protect and un-protect rearing; and the frequency of grooming in the light zone[119].

Radial maze (RM) test

The RM test was performed to measure working memory for spatial information. The maze was formed by eight arms, in which a stimulus was placed at the end of the Arm 8 during the training sessions. The stimulus was represented by a completely dark tube to mimic a safe place. To asses memory consolidation, the test was performed in two consecutive days: in day 1 animals were trained, while they were tested in day 2. To determine memory consolidation, animals' behavior was analyzed the day after their training trails (day 2). The mice were placed in the test room completely in the dark or dimly lit 1 hour before the start of the test. The training sessions (10 minutes each) were composed by four trials in which at each trial the animal was placed in the four cardinal arms. The day after, the mouse was placed in one of the cardinal arms. To assess the consolidation of spatial memory, we measured both the latency of entry and the time spent in Arm 8.

Three-chamber (3C) test

Mice (n=6-9 per condition) were subjected to the three-chamber test to assess their social tendency and long-term memory. The mice were placed in the test room completely in the dark or dimly lit 1 hour before the start of the test. The maze consisted of three chambers in which two transparent cylinders containing two different mice were located at the edges of the chambers. To asses memory consolidation, the test was performed in two consecutive days: in day 1 animals were trained, while they were tested in day 2. To determine memory consolidation, animals' behavior was analyzed the day after their training trails (day 2). During the training session, a *familiar* animal

was placed in one of the two cylinders. The tested mouse was placed in the middle chamber and was allowed to freely explore the three chambers. In day 2, two animals were placed under the two cylinders: the *familiar* one (old) and the *foreign* one (new). The tested mouse was placed in the middle chamber and was allowed to freely explore the three chambers. In this test, we evaluated several parameters: the cumulative duration of approaching the new and old animals, i.e., the total time spent near the two mice (sec); the frequency of interaction with the new and old animals, i.e., the frequency of the times the tested animal sniffs the two mice; the frequency of protect and un-protect rearing; and the frequency and the cumulative durations of grooming (sec). We considered also the Discrimination Index (DI), meaning the time spent exploring the *familiar* mouse relative to the total time spent exploring both animals [$(N_{new} - N_{old})/(N_{new} + N_{old})$, where N_{new} represents the frequency of the interaction with the new mouse, while N_{old} with the old one]. The resulting score ranges from -1 to +1, when positive, the animal interacts more with the *stranger* mouse, when negative with the old one. The interaction with the new mouse can also be expressed as a function of the Recognition Index (RI), which is the ratio of the amount of frequency exploring the *stranger* animal over the total frequency exploring both mice [$N_{new}/(N_{new} + N_{old})$] [120].

Passive avoidance (PA) test

This test was performed to assess emotional and long-term memory. In this test, animals (n=6-9 per condition) learned to avoid a previously administered aversive stimulus (such as a foot shake). The maze was elevated and consisted of two zones with a gate between the two: one zone completely in the dark, the other exposed to light and without barriers. To asses memory consolidation, the test was performed in two consecutive days: in day 1 animals were trained, while they were tested in day 2 and day 3. To determine memory consolidation, animals' behavior was analyzed the day after their training trails (day 2 and 3). Animals were placed in the light zone and allowed to explore both zones, but a mild (0.8 mA) foot-shock was administered when the animal entered the dark compartment. In day 2 and 3, to assess memory consolidation, mice were placed in the light zone again, and animals with normal learning and memory avoided entering the dark zone. This was measured by recording the latency to cross the gate between compartments and the frequency of entry attempts[121].

Immunofluorescence staining and microscopy

Briefly, the mice were anesthetized with a ketamine/xylazine mixture (80 mg/kg of ketamine and 10 mg/kg of xylazine) administered intraperitoneally. At this point the mice were first perfused with 0.9% NaCl and then with 4% paraformaldehyde (PFA). The drawn brains were left other 4 hours in PFA 4% for a post-fixation and then placed in 30% sucrose. The brains were then cut to

obtain 40 μm thick slices, then washed in PBS and incubated overnight with primary antibodies in PBS, Triton 2% and normal donkey serum 1.5% (017-000-121, Jackson ImmunoResearch). The primary antibodies used were: 6e10 (1:2000, 803001, BioLegend), AT8 (1:200, MN1020, Invitrogen), GFAP (1:3000, ab53554, Abcam), AQP4 (1:1500, HPA014784, Sigma Prestige), iba-1 (1:1000, 019-19741, Wako Chemicals), CD31 (1:500, 550300, BD Biosciences), c-Fos (1:1000, #2250, Cell Signaling Technology). The day after, the slices were washed again in PBS and incubated for 2 hours with secondary antibodies: CY3 conjugated AffiniPure donkey anti-rabbit or anti-goat IgG (1:400, 711-165-152 and 705-165-147, Jackson ImmunoResearch,), Alexa-Fluor488 conjugated AffiniPure donkey anti-mouse IgG (1:400, 715-545-151, Jackson ImmunoResearch), Alexa-Fluor647 conjugated AffiniPure donkey anti-rabbit IgG (1:400, 711-605-152, Jackson ImmunoResearch). For counterstaining, the brain sections were incubated with 4,6-diamidino-2-phenylindole (DAPI, 1:500, D9564, Sigma-Aldrich) and then washed with PBS. Finally, the slices were mounted on a glass slide and stored away from light and subsequently examined under the Leica TCS SP5 confocal laser scanning microscope (DM6000CS Leica) with 63x/1.40 oil objective, or the Zeiss Axioscan system Z.1 at a magnification of 10x (Plan-Apochromat, 10x/0.45 M27).

Image analysis in 5xFAD model

Regarding the regional analysis of the immunostaining, the slices were acquired with Zeiss Axioscan microscope. Each considered brain region was not fully analyzed, but we used brain slices (at least 3 slices per mouse) which differ by a minimum interval of distance from Bregma (lateral septum -1.045:1.420 mm; dentate gyrus, retrosplenial and motor-sensory cortex, thalamus, hypothalamus, and basolateral amygdala -2.255:-1.355 mm). All slices were compared to the Allen Mouse Brain Atlas (mouse.brain-map.org). The images were analyzed with Fiji (version 2.3.0/1.53q, Wayne Rasband, NIH, USA). The image analysis was carried out by measuring the percentage of pixels, after setting the same threshold for each different experiment for all regions of interest (ROIs). Each region has different sizes and since their dimensions can vary between slices, we used different ROIs (mean area for lateral septum~ 65941 μm^2, retrosplenial cortex~ 27887 μm^2, motor-sensory cortex~198789 μm^2, dentate gyrus~113222 μm^2, thalamus~215862 μm^2, hypothalamus~92535 μm^2, and basolateral amygdala~37553 μm^2).

As for colocalization analysis, we used a colocalization plugin of ImageJ, JaCoP[122]. the colocalization analyses were carried out with Manders' coefficient M1 and M2.

Microglia morphology analysis

As regards microglia, for each region we acquired three images per mouse (n=3 not fragmented, n=3 fragmented) with confocal microscope 63x/1.40 oil objective. To have statistical significance, we randomly chose three cells from those not associated with Aβ plaques, for a total of 27 cells per condition in each region (189 total cells per condition). To examine microglia morphology and study the complexity of cell structure, we analyzed the number of endpoints, junctions, and branches using AnalyzeSkeleton2D/3D plugin of ImageJ [123,124]. To the right of each iba1 image, the skeletons of the cropped cells are provided as a representation of the original image for each region analyzed.

Image analysis in wild-type model

The slices were firstly aligned to the Allen Mouse Brain Atlas by using the ABBA plugin of Fiji software (version 2.14.0/1.54f, Wayne Rasband, NIH, USA). The registered slices in the Atlas were then exported and analyzed in QuPath software (version 0.4.4)[125]. All the regions (annotations) of interest were analyzed by measuring the percentage of pixels, after setting the same threshold. As for c-Fos, the positive nuclei were counted manually.

Statistical analysis

Statistical analyses were performed using GraphPad Prism version 9.0 (GraphPad software, San Diego). All data are representative of the results of at least three independent experiments. All values were presented as mean ± standard error (SEM). Means were compared by t-test analysis or by one-way analysis of variance (ANOVA), in which adjusted *p* values were corrected for multiple testing using the Bonferroni *post hoc* test. In both statistical analyses, p value < 0.05 was defined to be significant. As regards the EEG analysis, the hypnograms (sleep and wake periods during a day) obtained in normal conditions and during SF were visually compared in order to confirm the efficacy of the protocol.

Results

Validation of SF protocol through electroencephalography (EEG) recordings

As stated in methods section, the aim of our SF protocol was to achieve a chronic state of SF for 30 days, without significantly impairing the total amount of sleep (Fig. 4A). The hypnograms obtained in normal conditions and during SF periods were analyzed and as expected, both the wild type (wt) and the 5xFAD strains showed a significant increase of sleep/wake shifts (Fig. 4B). A mild decrease (10-25%) in the total sleep time (TST) during the 24h recording was observed during SF period when compared to normal conditions (Fig. 4C), but such values are similar to normal data reported in literature for animals of the same age (the TST in *Mus musculus* strain BL6 ranges from 34.7% to 45.4% [126], 5% in C57BL/6N mice [127], for C57BL/6 strain approximately the 48.9% [128]). Although 5xFAD mice already display sleep alterations in comparison to wt animals, in both genotypes we noticed a decrease in NREM sleep during fragmentation and, conversely, an increase in the waking period, while REM sleep remains virtually unchanged, confirming our fragmentation protocol (Fig. 4D).

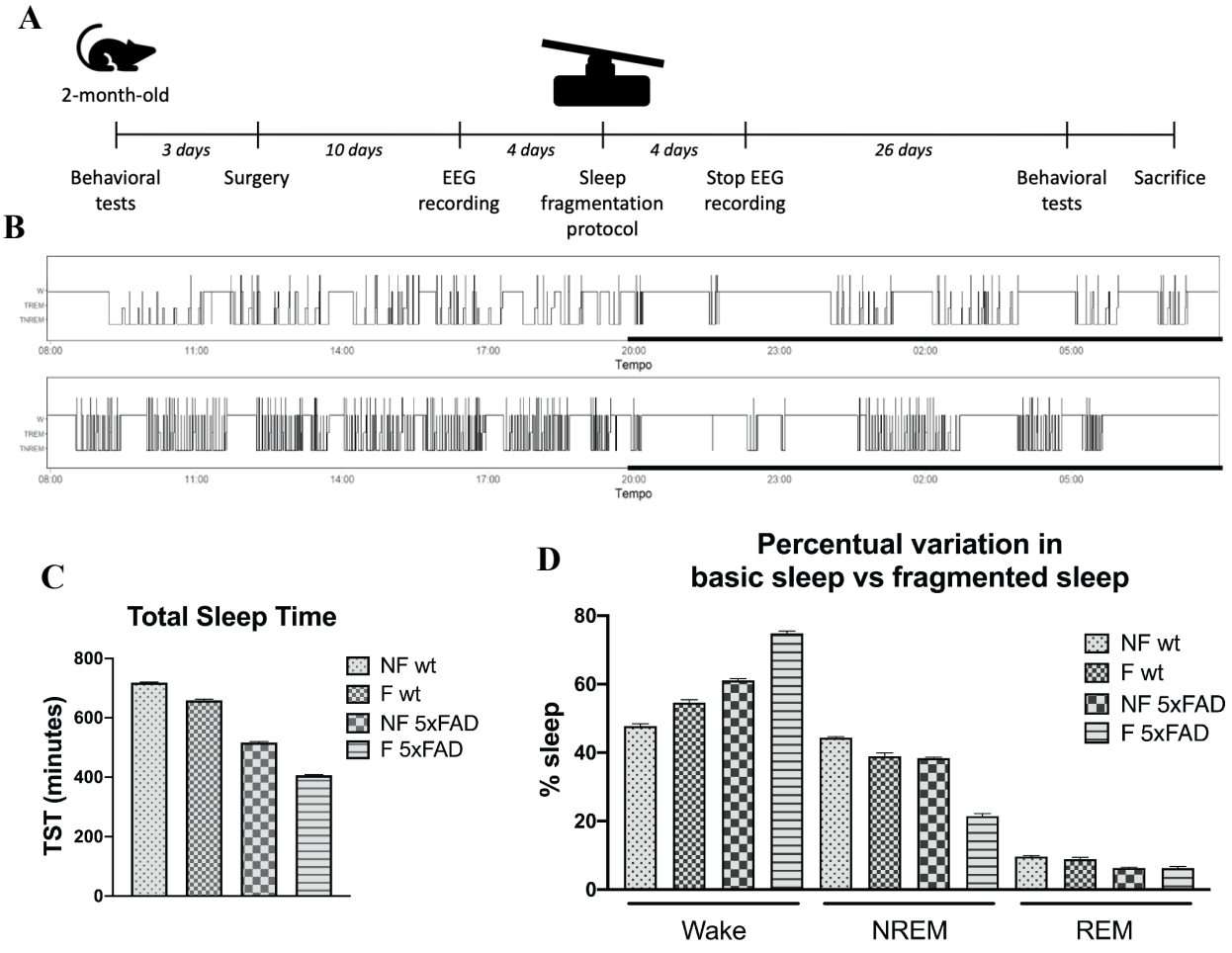

Figure 4. A SF protocol time-line. **B** Typical hypnograms reporting sleep oscillations during baseline 24h recording (top) and during fragmentation protocol (bottom). Thick lines indicate the dark period. **C** Total sleep time is represented as an average of the recordings. **D** The variation in the percentages relating to wakefulness, NREM sleep, and REM sleep. The two genotypes were compared for the three variables in basal and fragmentation conditions. NF=not fragmented mice; F=fragmented mice. The data are mean standard error of the mean (SEM), n=3 per strain.

Sleep fragmented 5xFAD mice show an accentuated anxious behavior analyzed by the EPM and the OF tests

As shown in Figure 2A and B, SF had different effects on anxious and hyperactive behavior in the EPM test. The t-test analysis revealed increased anxiety in fragmented (F) 5xFAD mice by reducing the time spent in the open arms compared with not fragmented (NF) 5xFAD (Fig. 5A). Furthermore, SF enhanced anxiety by increasing hyperactivity as shown in the total distance traveled in arena, which is greater in the closed arms than in the open ones (Fig. 5B). About the total time spent in the arena exploration, the F-5xFAD group showed an increase in the anxious behavior in the OF that led the animals to spend more time on the edges of the apparatus and less in the center than controls (Fig. 5C). In addition, the F-5xFAD group showed an increase in motor activity in the edges (Fig. 5D) and in the frequency of protected rearing (Fig. 5E), along with a reduction in motor activity in the center (Fig. 5C) and in the frequency of unprotected rearing (Fig. 5D) compared with the NF-5xFAD group.

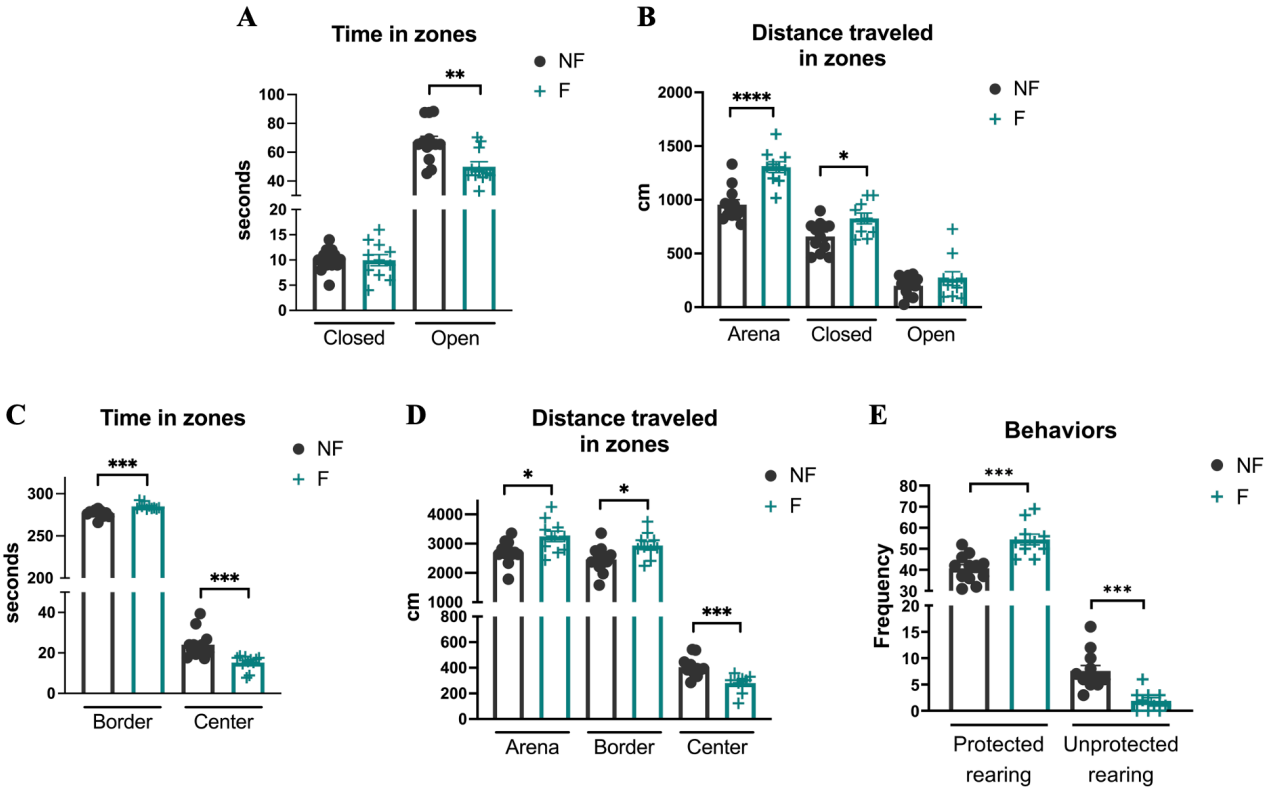

Figure 5. A Time spent in both closed and open arms during the EPM test. **B** Distance traveled in closed and open arms, and in the total arena during the EPM test. **C** Distance traveled in arena, border, and center in the OF test. **D** Time spent in both the border and the center of the arena during the OF test. **E** Behavioral activities during the OF test (protective and un-protective rearing). NF=not fragmented mice; F=fragmented mice. The data are mean standard error of the mean (SEM). Each data point represents an individual animal. ns=not significant; *p<0.05; **p<0.01; ***p<0.005; ****p<0.0001 versus control by t-test analysis, n=11 per condition.

SF impairs object recognition memory during the NOR test in 5xFAD mouse model

In this behavioral test, sleep disruption affected object recognition memory in 5xFAD animals (Fig. 6A). Indeed, SF reduced the interaction with the new and the old object (Fig. 6B), suggesting a compromised short-term memory. This finding confirmed with further analyses, in which the discrimination (Fig. 6C) and recognition indexes (Fig. 6D) are reduced after SF.

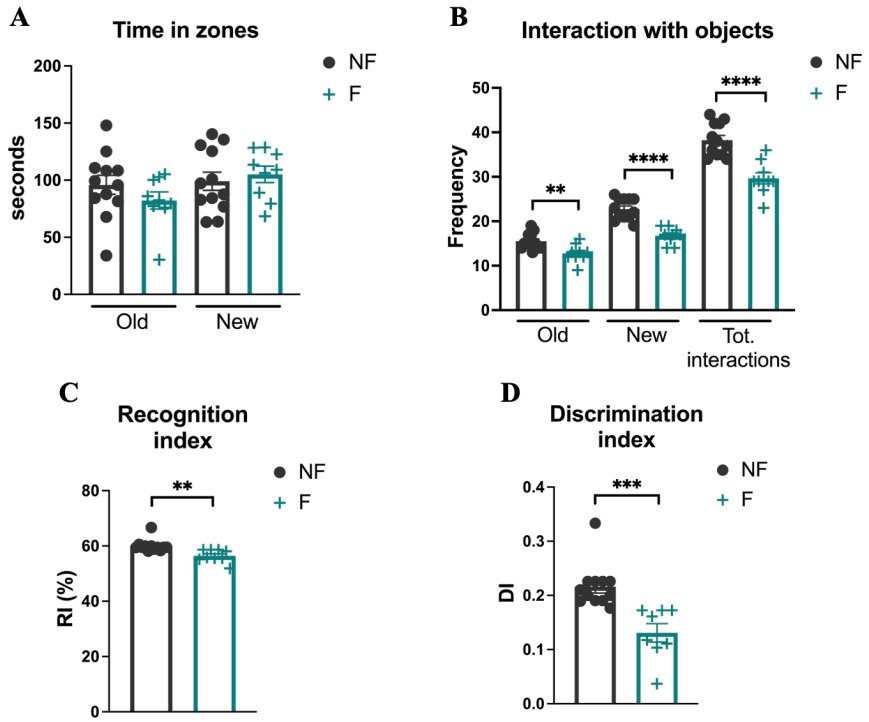

Figure 6. A Time spent near the old and the new objects. **B** Interaction with the old and the new objects and the total frequency of interaction with both objects. **C** and **D** Respectively recognition index percentage and the discrimination index. NF=not fragmented mice; F=fragmented mice. The data are mean standard error of the mean (SEM). Each data point represents an individual animal. ns=not significant; **p<0.01; ***p<0.005; ****p<0.0001 versus control by t-test analysis, n=11 per condition.

SF impairs spatial memory during the Y-maze test in 5xFAD mice

We examined the impact of disrupted sleep patterns on both working and spatial memory using the Y-maze test. F-5xFAD group displayed a decrease in the percentage of alternation and maximal alternation entries within the arms of the maze. This decline indicated memory impairment when compared with the control group (see Fig. 7A). The percentage of alternation correlated with the animal's movement within the maze (Fig. 7B) and the time it spent in the arms (Fig. 7C). In fact, the F-5xFAD group covered a shorter distance within the maze (Fig. 7B), remained longer in the new arm (Arm 3; Fig. 7C), and took more time to reach it compared with the control group (Fig. 7D). Additionally, memory impairment can be evaluated by examining how often the animal

reentered an arm it had previously visited, either directly or indirectly. These two factors are linked to the overall number of arm entries and, by extension, exploration. The F-5xFAD group demonstrated a reduced total frequency of arm entries (Fig. 7A) compared with the control group, which decreased the number of times they directly reentered the initial arm (Fig. 7E). This suggests a diminished ability for exploration.

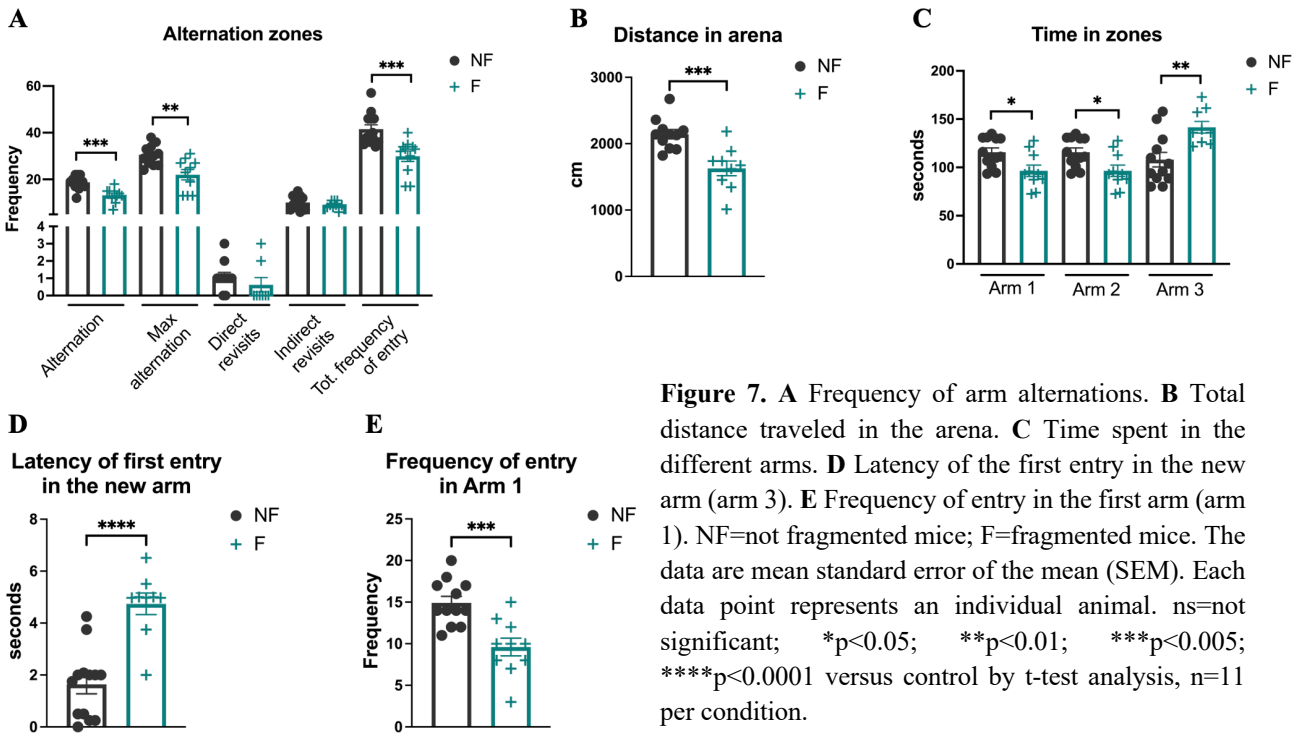

Figure 7. A Frequency of arm alternations. **B** Total distance traveled in the arena. **C** Time spent in the different arms. **D** Latency of the first entry in the new arm (arm 3). **E** Frequency of entry in the first arm (arm 1). NF=not fragmented mice; F=fragmented mice. The data are mean standard error of the mean (SEM). Each data point represents an individual animal. ns=not significant; *p<0.05; **p<0.01; ***p<0.005; ****p<0.0001 versus control by t-test analysis, n=11 per condition.

SF accelerates AD progression by enhancing Aβ accumulation and inducing tau phosphorylation in 5xFAD mice

As for 5xFAD mice, this strain at 2 months of age already displays visible extracellular Aβ accumulation, thus we explored whether this accumulation could be more emphasized after sleep disruption. As shown in Figure 8A, in F-5xFAD mice compared with control, Aβ accumulation increased in both the cortexes and the dentate gyrus, as well as in most of the other regions also involved in sleep regulation (Fig. 8B, C). Interestingly, Aβ accumulation increased also in the lateral septum (data not shown), a brain region which modulates cognitive processing in the cortex and hippocampus. We also observed an initiation of tau phosphorylation in the dentate gyrus in 5xFAD mice after SF compared with the not F-mice, where tau phosphorylation is not observed (Fig. 8D).

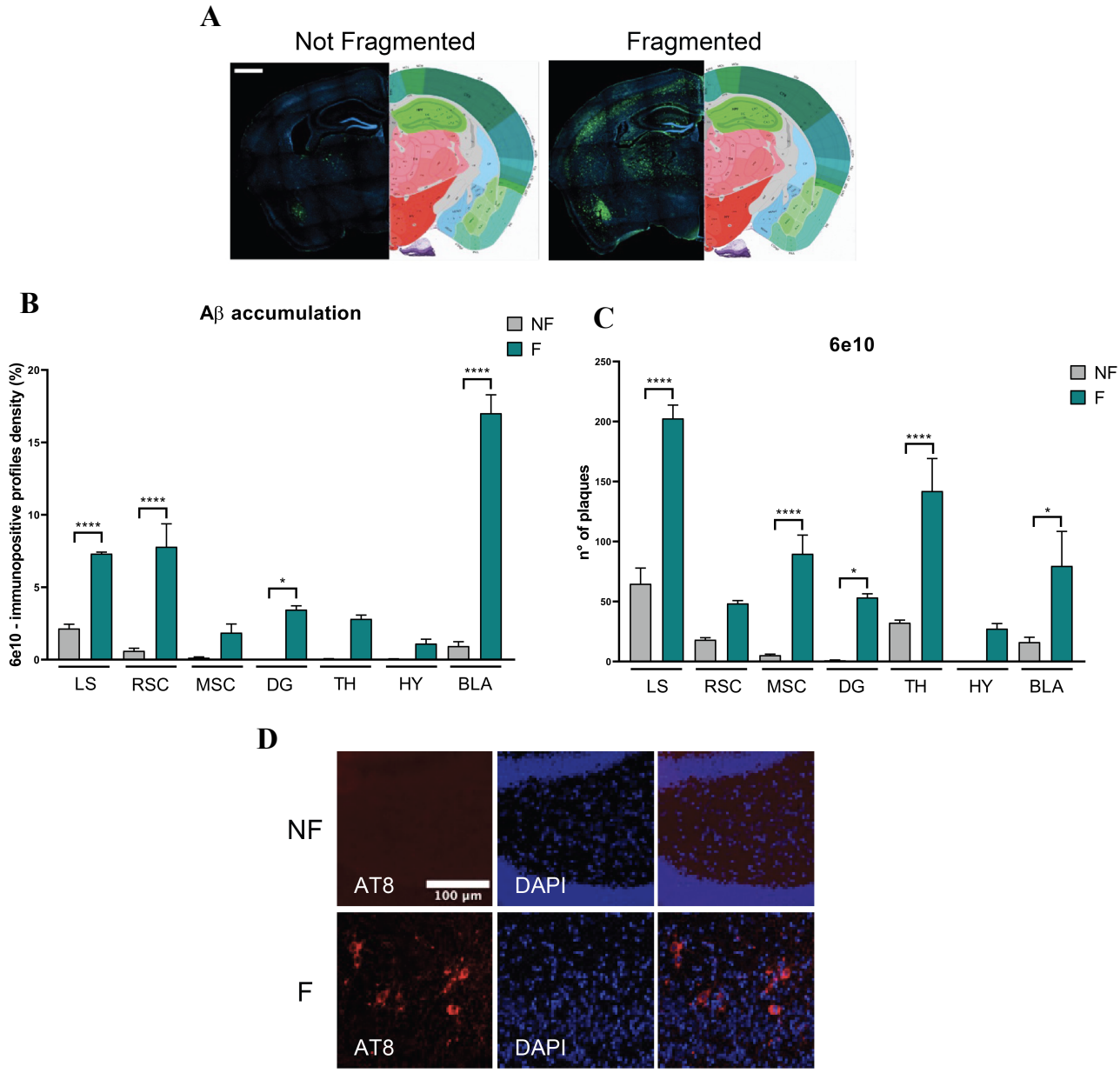

Figure 8. A Representative image of immunohistochemistry of 6e10 antibody. Scale bar 1000 µm. Aβ plaques are labeled in green and the nuclei with DAPI in blue. **B** Histogram of 6e10 density. **C** Histogram of Aβ plaque number. **D** Representative image of immunohistochemistry of AT8 antibody. NF=not fragmented mice; F=fragmented mice. LS=lateral septum; RSC=retrosplenial cortex; MSC=motor-sensory cortex; DG=dentate gyrus; TH=thalamus; HY=hypothalamus; BLA=basolateral amygdala. The data are mean standard error of the mean (SEM). *p<0.05; ****p<0.0001 versus control by one-way ANOVA followed by Bonferroni *post-hoc* test, n=4 per condition.

SF induces neuroinflammation by activating microglia and consequently astrocytes

Neuroinflammation is known to occur in AD pathology. To validate an activation of the neuroinflammation mediated by sleep disruption, we analyzed by immunofluorescence the density of astrocyte cells. GFAP+ signal increased in all the areas analyzed in F-5xFAD mice compared with control, thus indicating a possible astrogliosis (Fig. 9A-D). This signal well correlates with the increase of Aβ plaque accumulation (Fig. 9C). To confirm this result, we investigated microglia activation, which is known to activate astrocytes by the release of immune factors. We observed a major activation of microglia in F-5xFAD mice compared with control (Fig. 10A). This activation is notable by analyzing microglia morphological complexity by AnalyzeSkeleton(2D/3D) ImageJ plugin (Fig. 10B-H). In F-5xFAD mice, iba1+ cells are more activated by comparing the number of cell branches, branch junctions, and the voxel end-points which significantly decreased in most of the regions analyzed compared with control, in which microglia cells are less activated and consequently more ramified.

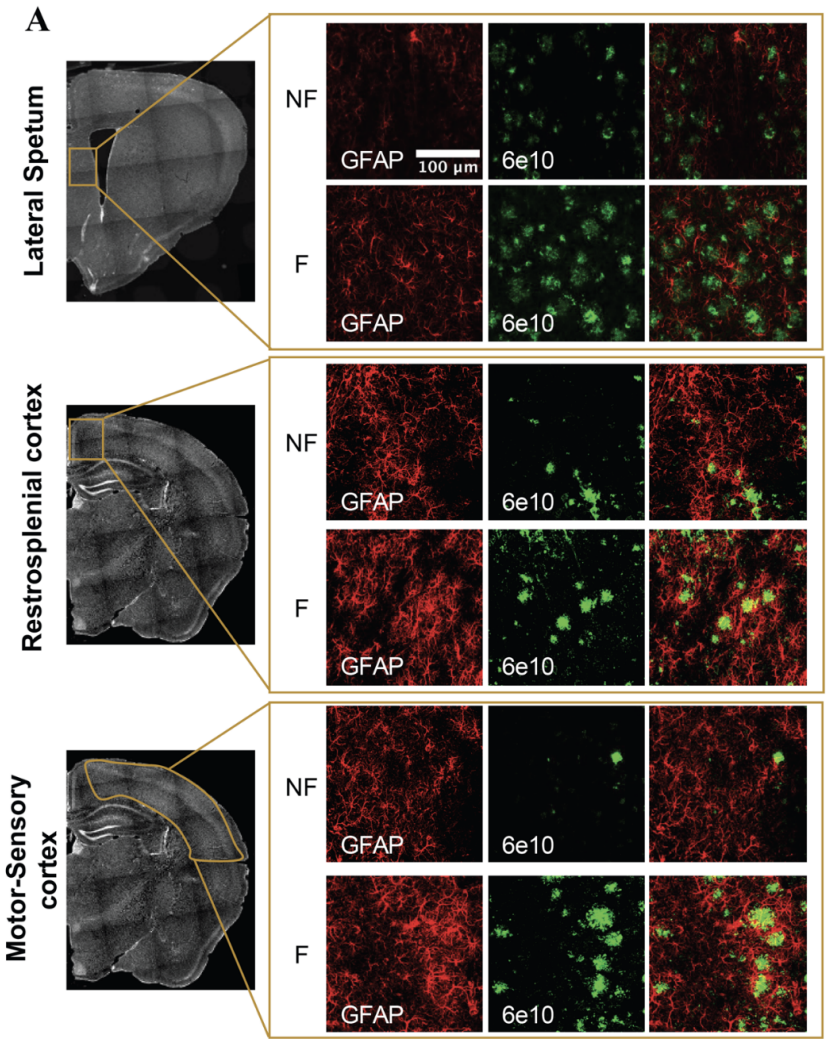

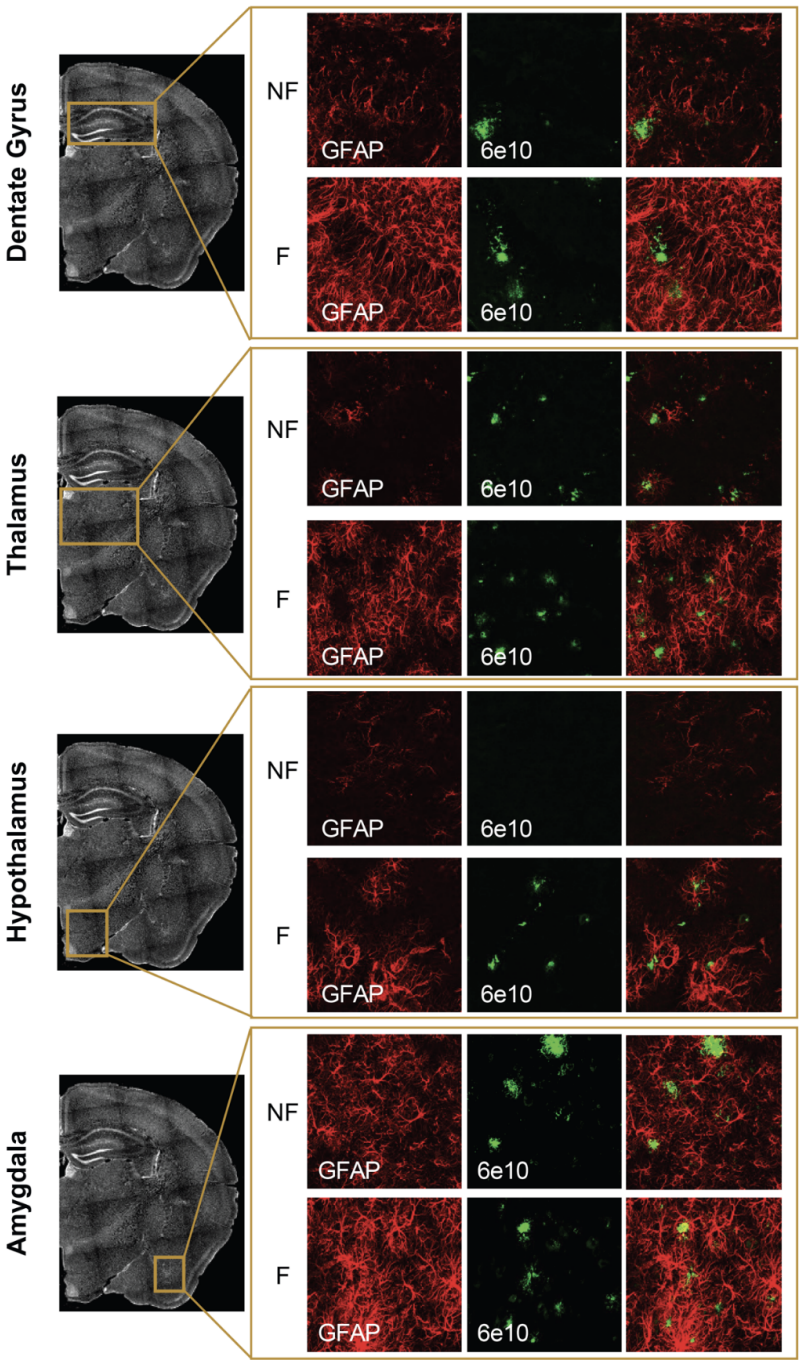
Dentate Gyrus
Thalamus
Hypothalamus
Amygdala
NF
F
GFAP
6e10

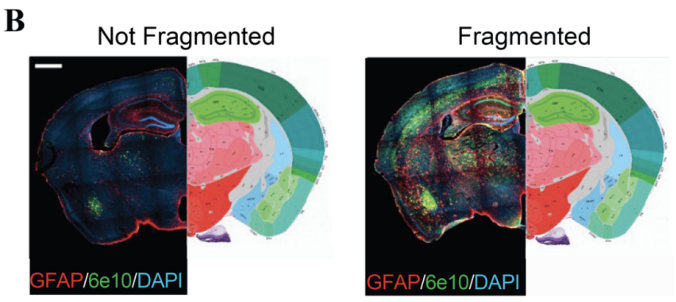
B
Not Fragmented
Fragmented
GFAP/6e10/DAPI
GFAP/6e10/DAPI

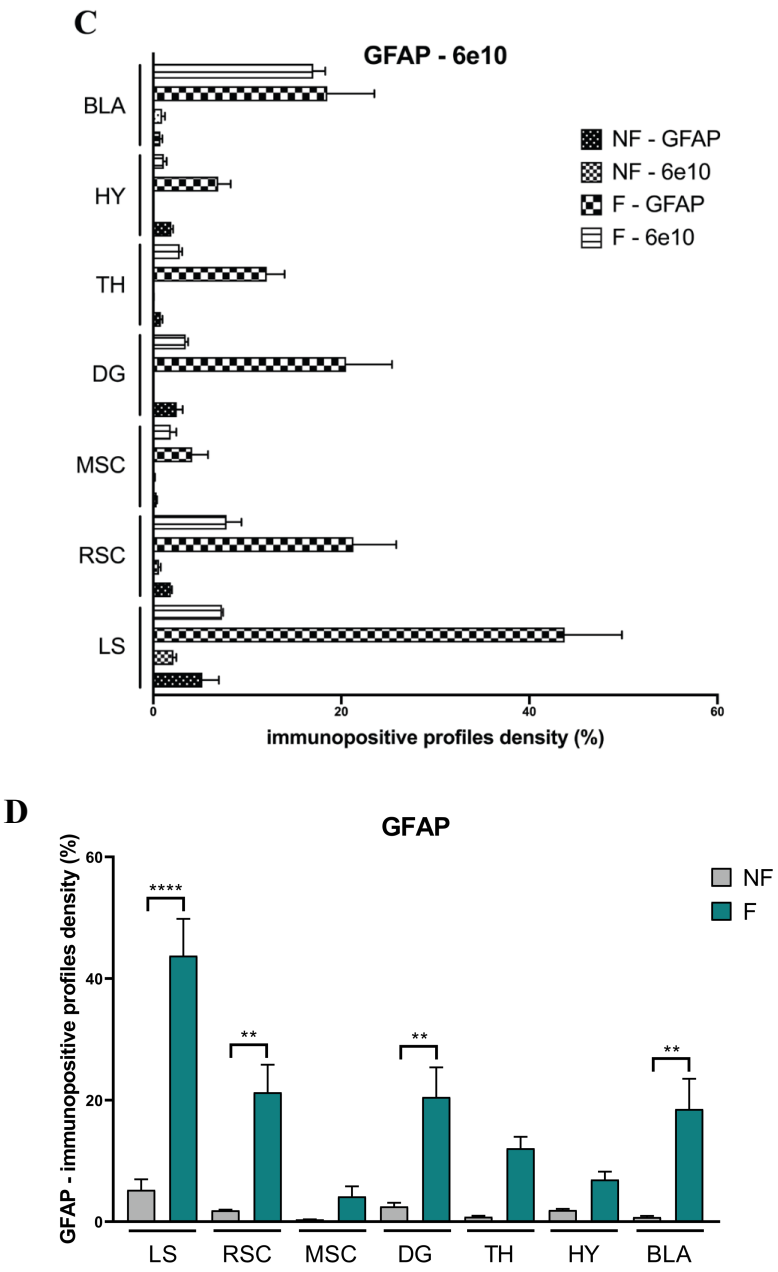

Figure 9. A Representative image of immunohistochemistry of GFAP and 6e10 antibodies in all the regions analyzed. **B** Representative image of immunohistochemistry of GFAP and 6e10 antibodies. Scale bar 1000 μm. **C** Histogram of GFAP and 6e10 densities showed together. **D** Histogram of GFAP density. NF=not fragmented mice; F=fragmented mice. LS=lateral septum; RSC=retrosplenial cortex; MSC=motor-sensory cortex; DG=dentate gyrus; TH=thalamus; HY=hypothalamus; BLA=basolateral amygdala. The data are mean standard error of the mean (SEM). **p<0.01; ****p<0.0001 versus control by ANOVA followed by Bonferroni *post-hoc* test, n=4 per condition.

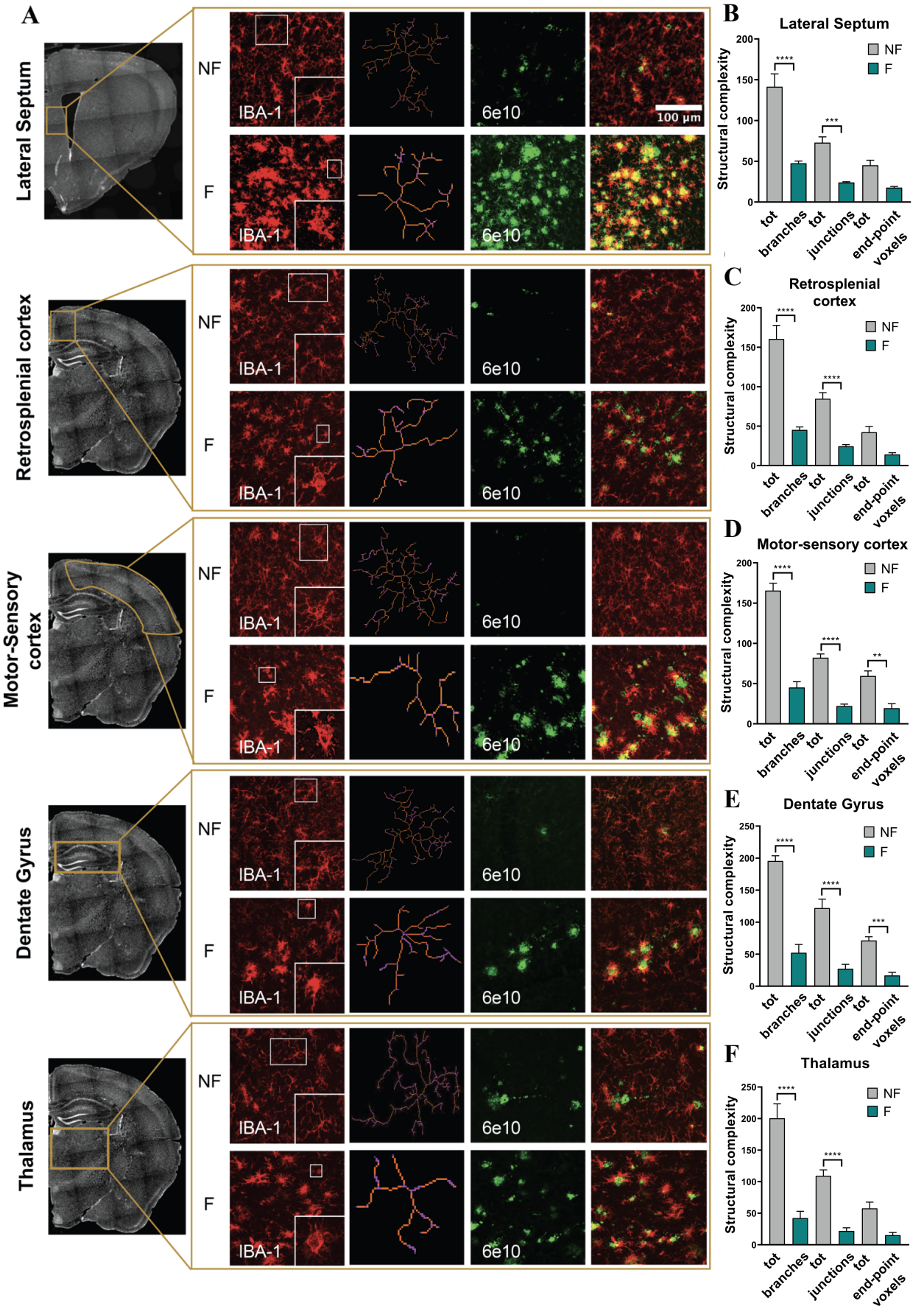
A
Lateral Septum
Retrosplenial cortex
Motor-Sensory cortex
Dentate Gyrus
Thalamus
NF
F
IBA-1
6e10
100 µm
B
Lateral Septum
C
Retrosplenial cortex
D
Motor-sensory cortex
E
Dentate Gyrus
F
Thalamus
Structural complexity
NF
F
tot branches
tot junctions
tot end-point voxels

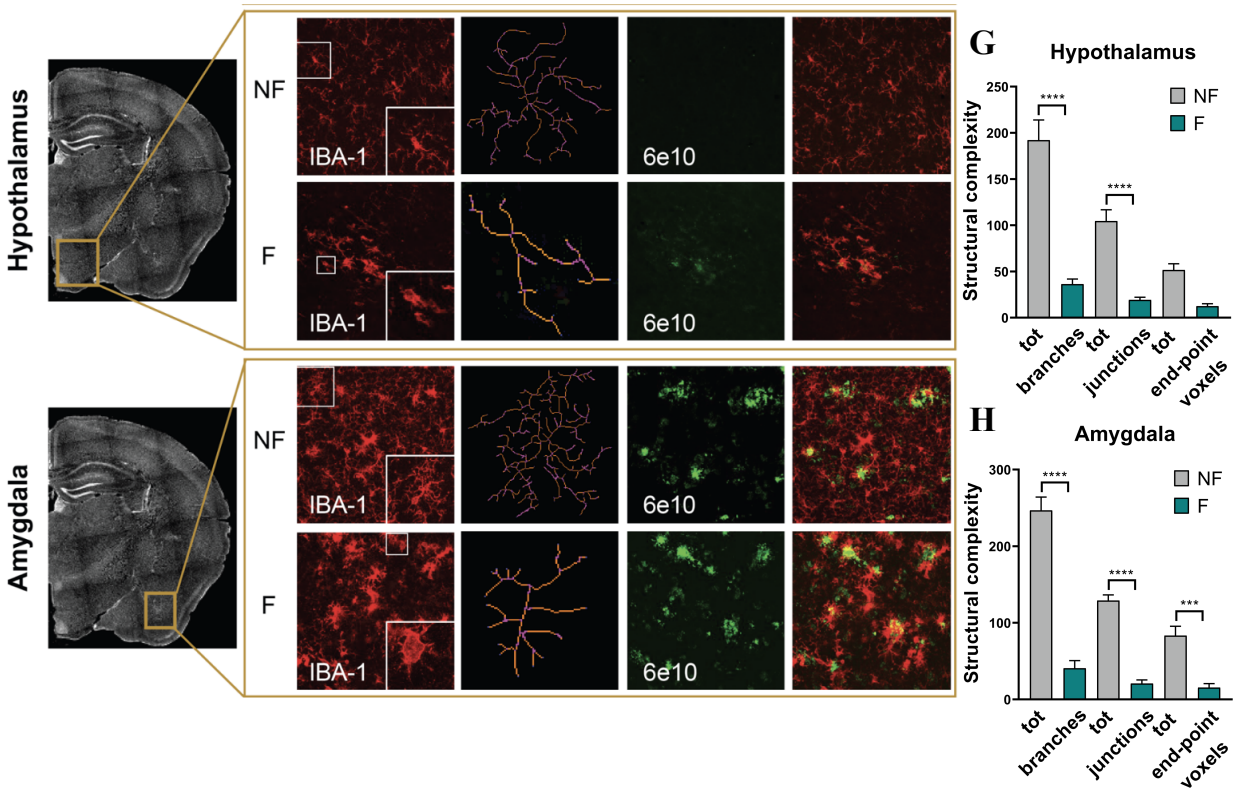

Figure 10. A Representative image of immunohistochemistry of iba-1 and 6e10 antibodies. A representation of skeletonized cells is shown on the right of iba-1 images. **B-H** Analysis of the structural complexity of microglia cells. NF=not fragmented mice; F=fragmented mice. The data are mean standard error of the mean (SEM). **p<0.01; ***p<0.005; ****p<0.0001 versus control by ANOVA followed by Bonferroni *post-hoc* test, n=3 per condition.

SF differently influences AQP4 expression according to the severity of the disease

One of the clearance pathways of Aβ plaques is displayed by the glymphatic system, in particular by the activity of the AQP4 channel, located in the end-feet of astrocytes surrounding vessels. Since we observed an augmentation of Aβ accumulation mediated by sleep disruption, we investigated whether this clearance system is compromised. In 2-month-old 5xFAD mice, we observed an increase in the density of AQP4+ signal in all the brain areas involved (Fig. 11A, B). But despite the augmentation of Aβ plaques, we detected the AQP4 signal in the perivascular areas in both the control and the fragmented mice, thus indicating a possible functional channel activity (Fig. 11C). Notably, AQP4 colocalized with GFAP signal (Fig. 12A, B), thus confirming that AQP4 increase is determined by its expression rather than its release in the CSF. Interestingly, in older mice (6-month-old) we observed a decrease of AQP4+ signal (Fig. 11D, E), which could be due to a decrease in astrocyte cells. But when analyzing the density of astrocyte cells, we did not observe any significant change in the amount of GFAP+ signal (Fig. 11F).

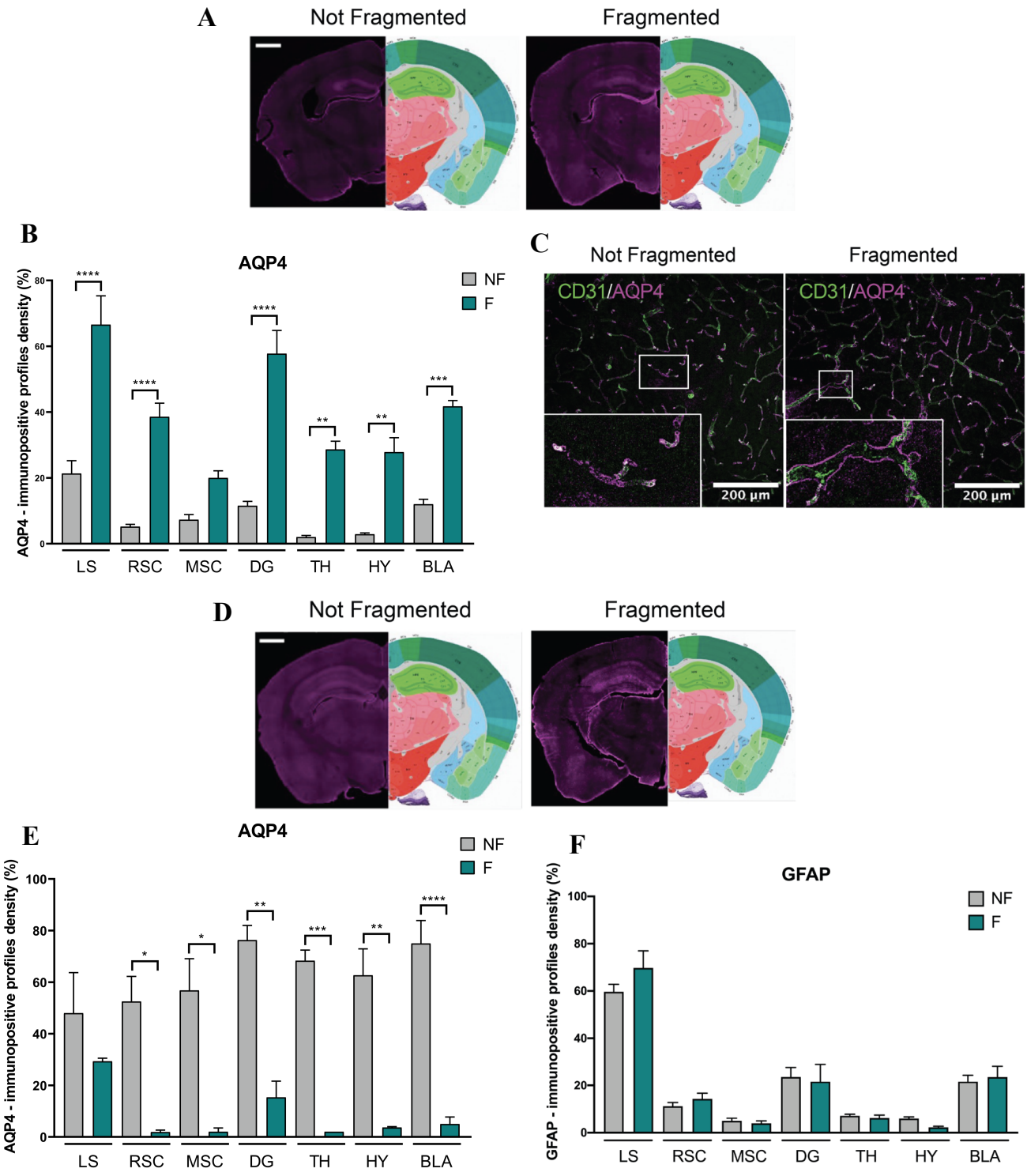

Figure 11. A Representative image of immunohistochemistry of AQP4 antibody in 2-month-old mice. Scale bar 1000 µm. **B** Histogram of AQP4 density in 2-month-old mice. **C** Representative image of immunohistochemistry in 2-month-old mice of AQP4 and CD31, blood vessel marker. **D** Representative image of immunohistochemistry of AQP4 antibody in 6-month-old mice. Scale bar 1000 µm. **E** and **F** respectively, histograms of AQP4 and GFAP densities in 6-month-old mice. NF=not fragmented mice; F=fragmented mice. LS=lateral septum; RSC=retrosplenial cortex; MSC=motor-sensory cortex; DG=dentate gyrus; TH=thalamus; HY=hypothalamus; BLA=basolateral amygdala. The data are mean standard error of the mean (SEM). *p<0.05; **p<0.01; ***p<0.005; ****p<0.0001 versus control by ANOVA followed by Bonferroni *post-hoc* test, n=4 per condition.

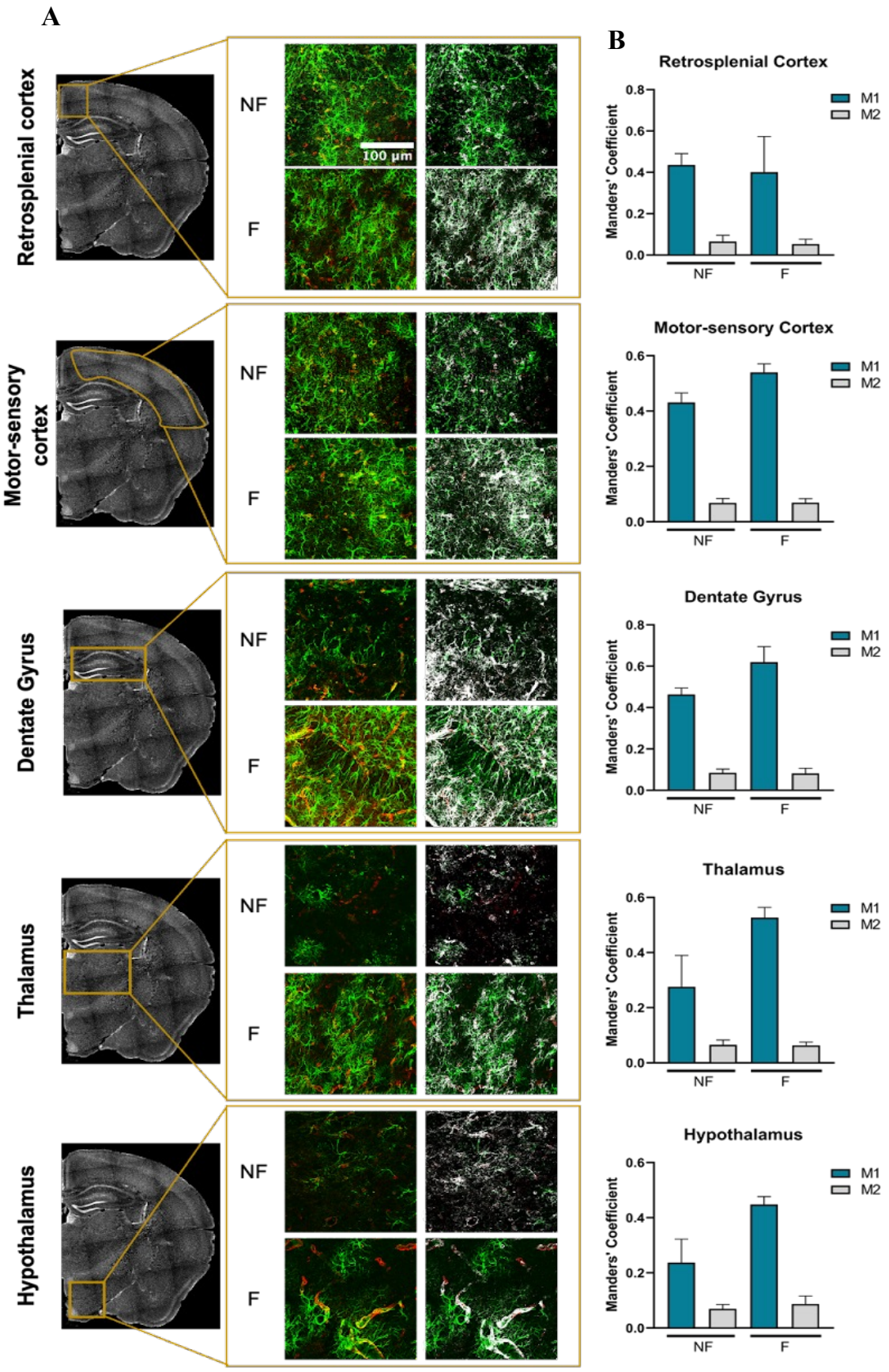
A
B
Retrosplenial cortex
Motor-sensory cortex
Dentate Gyrus
Thalamus
Hypothalamus
NF
F
100 µm
Retrosplenial Cortex
Motor-sensory Cortex
Dentate Gyrus
Thalamus
Hypothalamus
Manders' Coefficient
0.0
0.2
0.4
0.6
0.8
M1
M2
NF
F

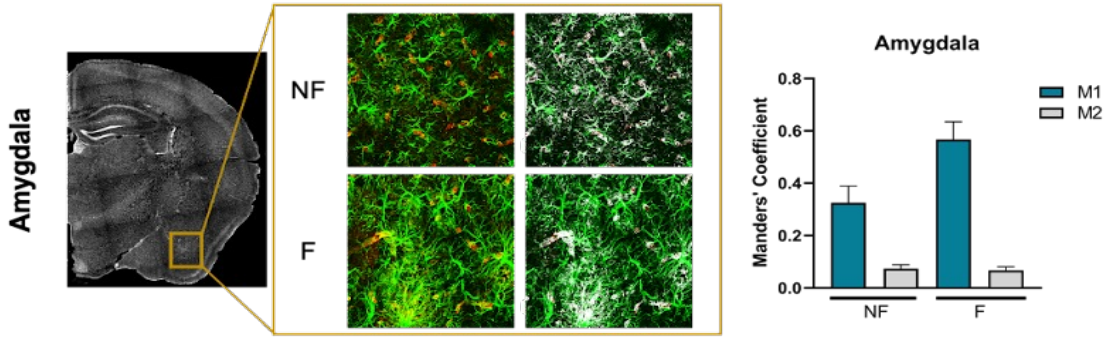

Figure 12. A Representative image of immunohistochemistry of GFAP and AQP4 antibody colocalization in the different brain areas. GFAP staining in green and AQP4 staining in red. In the right, the respective colocalization masks, with colocalizing pixels in withe. **B** Histograms of colocalization analysis which was carried out with Manders' coefficients M1 and M2. M1 represents AQP4-related pixels overlapping with GFAP signal, while M2 describes GFAP-related pixels overlapping with AQP4 signal. NF=not fragmented mice; F=fragmented mice. The data are mean standard error of the mean (SEM) and they were analyzed by ANOVA followed by Bonferroni *post-hoc* test, n=3 per condition.

SF causes stress-like behavior in wild-type animals

We evaluated the effect of SF in wild-type (wt) animals too. Particularly, we focused on the same behavioral paradigms already analyzed in 5xFAD mouse model. In the EPM test, fragmented wild-type (F-wt) mice spent more time in both arms (Fig. 13A), thus showing stress-like behavior with elevated motor activity even in the open arms compared with the control (Fig. 13B). In the OF test, F-wt animals showed a significative reduction in the frequency of unprotected rearing (Fig. 13E), again emphasizing this anxious behavior observed in the EPM. Furthermore, SF impaired animal ability to discriminate and evaluate a potentially dangerous situation from a safe one in the light-dark (LD) test. In fact, the F-wt group was exposed more frequently and longer in the light zone (Fig. 13F, G), thus increasing the possibility of being predated. In contrast, the control group showed preserved survival behavior (Fig. 13H).

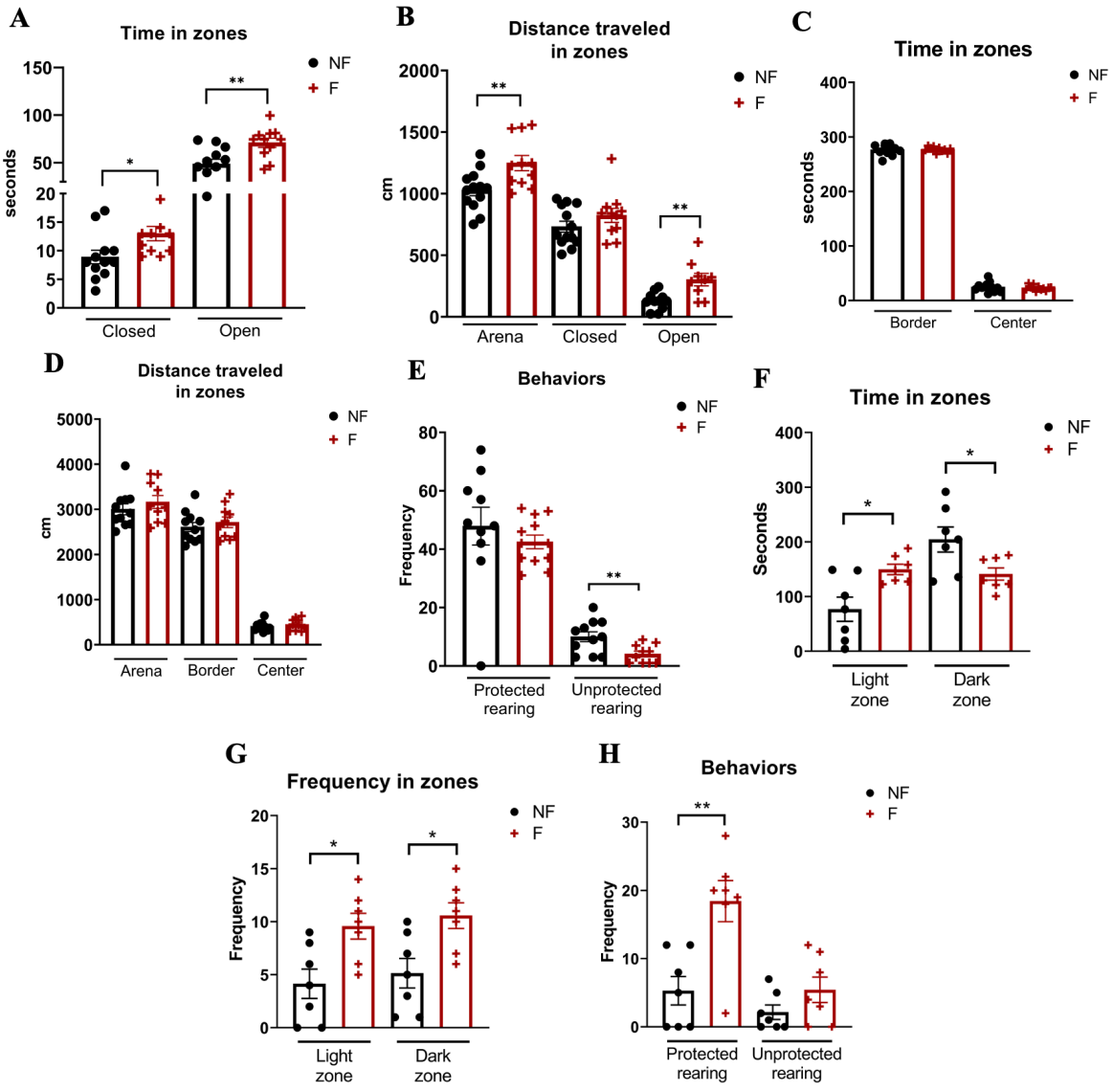

Figure 13. A Time spent in both closed and open arms during the EPM test. **B** Distance traveled in closed and open arms and in the total arena during the EPM test. **C** Distance traveled in arena, border, and center in the OF test. **D** Time spent in both the border and the center of the arena during the OF test. **E** Behavioral activities during the OF test. **F** and **G** Respectively, the time spent and the frequency in both light and dark zones during the LDT test. **H** Behavioral activities during the OF test. NF=not fragmented mice; F=fragmented mice. The data are mean standard error of the mean (SEM). Each data point represents an individual animal. ns=not significant; *p<0.05; **p<0.01 versus control by t-test analysis, n=11 (EPM and OF) and n=7 (LDT) per condition.

SF compromises the object recognition memory in wild-type mice

As shown in Fig. 14, F-wt animals spent less time in the old object rather than in the new one compared with controls (Fig. 14A), but their total interaction with both objects is reduced respect to controls (Fig. 14B). Moreover, the two indexes of object recognition and discrimination were reduced in F-wt animals compared with controls (Fig. 14C, D). This decrease in object interaction may be due to increased stress after SF.

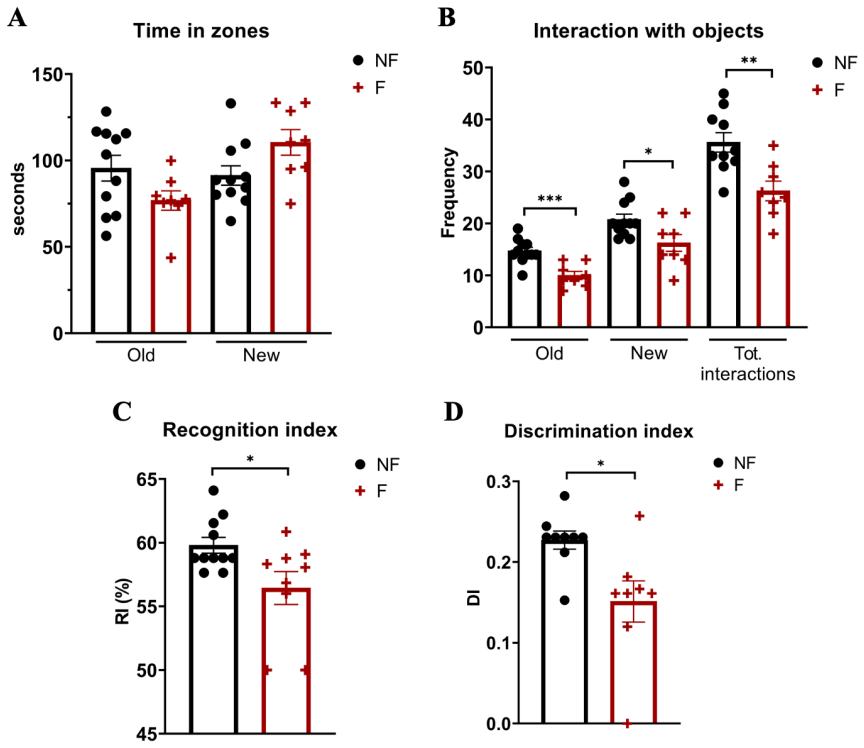

Figure 14. A Time spent near the old and the new objects. **B** Interaction with the old and the new objects and the total frequency of interaction with both objects. **C** and **D** Respectively, recognition index percentage and the discrimination index. NF=not fragmented mice; F=fragmented mice. The data are mean standard error of the mean (SEM). Each data point represents an individual animal. ns=not significant; *p<0,05; **p<0,01 versus control by t-test analysis, n=11 per condition.

Memory consolidation fails as a result of SF in the wt-type strain

Since several data report that memory consolidation occurs during NREM sleep, which is disrupted in our experimental protocol (Fig. 4D), we investigated whether it may be altered in our model. To asses memory consolidation, we performed a series of tests, during which we observed that SF had a detrimental effect on memory consolidation. This was determined by analyzing animals' behavior the day after their training trails. Specifically, we evaluated the working memory (procedural memory) and problem-solving capabilities through the puzzle box (PB) test. In this behavioral paradigm, F-wt mice exhibited a prolonged search for the gallery, made more errors, and spent more time compared to the control group (Fig. 15A, B). In addition, employing the previously described discrimination indexes, the F-wt group displayed lower discrimination indexes (Fig. 15C, D), indicating impairment in cognitive functions related to working memory. Another type of procedural memory, the spatial memory, was assessed using the radial maze (RM) test. We

observed that this form of working memory was also compromised in animals subjected to SF protocol. Notably, contrary to the control group, F-wt mice remained less time and took longer in reaching the Arm 8 (fig. 15E, F), in which the stimulus had been presented the day before. Given our observation of anxious and highly stressed behavior in F-wt animals during tests such as the EPM, OF, and LD, we decided to explore other types of memory that are related to amygdalar nuclei, specifically emotional memories[129]. Consequently, we noted a hindered consolidation of this type of memory in SF group. In particular, in the three-chamber (3C) test, F-wt animals showed reduced cognitive abilities in discriminating a familiar social stimulus from a new one. In fact, unlike the control group, the F-wt mice failed to recognize the animal they had interacted with the previous day, as evidenced by the discrimination indexes (Fig. 15G-J). Finally, we evaluated the consolidation of contextual fear memory through the passive avoidance (PA) test. This test allowed us to assess long-term memory by performing it one and two days after the training session. Interestingly, SF did not alter the consolidation of this specific type of memory associated with a negative event, such as the foot shock stimulus. Indeed, both groups, which have been exposed to the same negative stimulus the previous day, did not exhibit a significant difference in entry latency into the apparatus either one or two days after training (Fig. 15K). Notably, the control group never entered or attempted to enter the apparatus containing the negative stimulus (Fig. 15K, L), in contrast to F-wt animals, of which 42% attempted entry one day after training and 28% attempted entry two days after training (Fig. 15L).

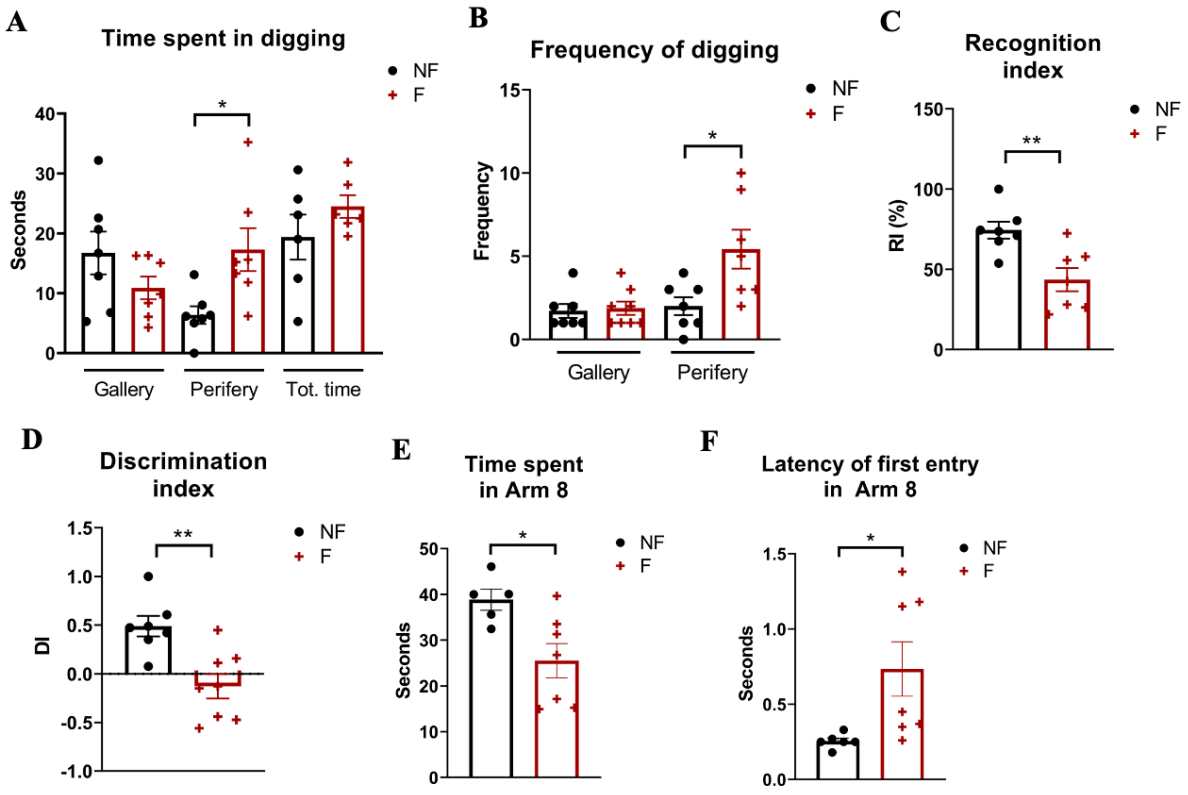

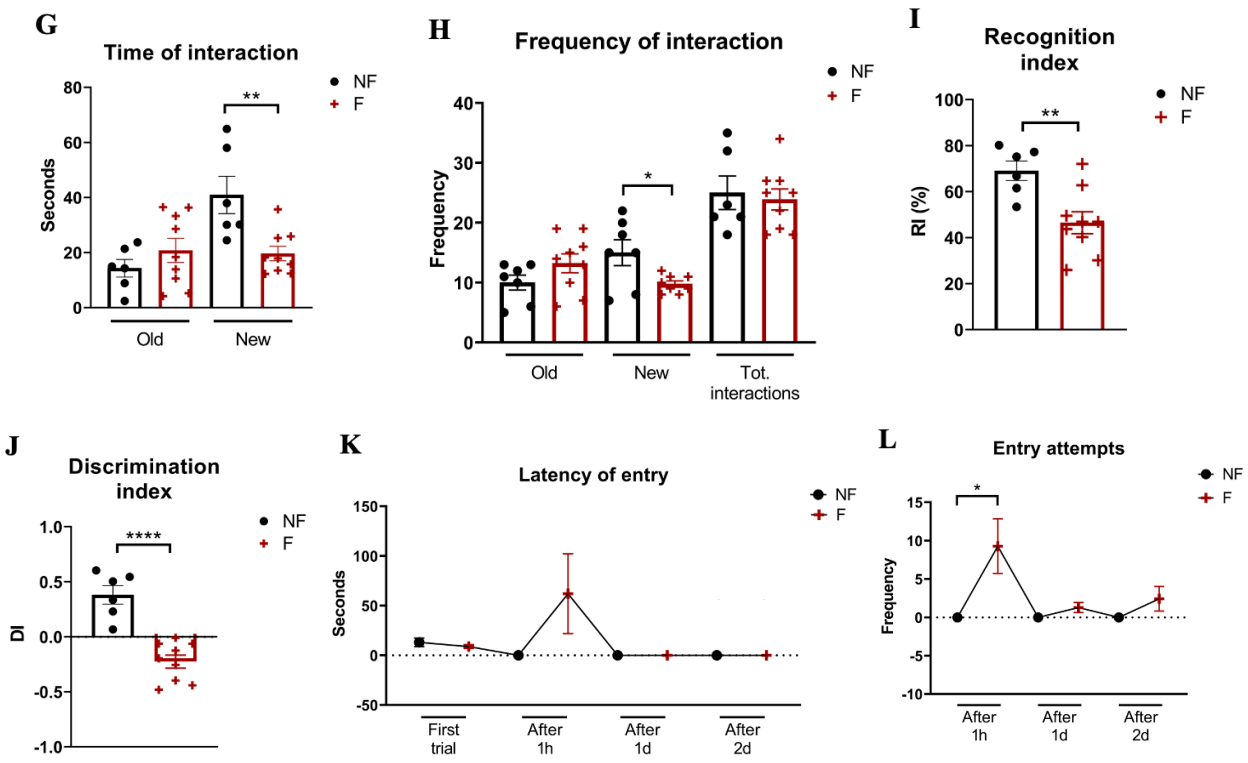

Figure 15. A and **B** Respectively, the time spent in and the frequency of digging during the PB test. **C** and **D** Respectively, recognition index percentage and discrimination index in the PB test. **E** and **F** Respectively, the time spent in and the latency to reach out Arm 8 (with the stimulus) in the RM test. **G** and **H** Respectively, the interaction time and the frequency of approaching with both the old and the new animals during the 3C test. **I** and **J** Respectively, recognition index percentage and discrimination index in the 3C test. **K** and **L** Respectively, the latency and the attempts of entry in the dark zone (with the foot shock stimulus) in the PA test. NF=not fragmented mice; F=fragmented mice. The data are mean standard error of the mean (SEM). Each data point represents an individual animal. ns=not significant; *p<0.05; **p<0.01; ****p<0.0001 versus control by t-test analysis, n=7 per condition.

Sleep disruption may affect the glymphatic system by decreasing AQP4 levels in wild-type mice

Since several data report that a deficiency in the expression of AQP4 channel led to a defect in synaptic plasticity, learning, and memory [130,131] and given our findings on behavioral tests, we investigated whether the glymphatic system is affected by SF. Indeed, we observed a significant decrease in the levels of AQP4+ signal after SF in the amygdala and the dentate gyrus (Fig. 16A, B), the two regions involved in learning, memory, and sleep regulation. Moreover, to better understand whether this data could be related to a possible astrocyte cell death, we also analyzed GFAP-signal density, which did not significantly change after SF (data not shown). In addition, we further investigated whether this decrease in AQP4 must be subregion specific. In fact, we observed that AQP4+ signal decreased in the entire hippocampus, particularly in the granule cell layer (sg) of the dentate gyrus (DG), CA1 and CA3 subregions (Fig. 16D, E). Moreover, in the

amygdala, AQP4+ signal is reduced in all the three amygdalar nuclei examined, such as lateral (LA), basolateral (BLA), and basomedial (BMA) amygdala (Fig. 16C, E). Again, this data did not correlate with GFAP loss (data not shown).

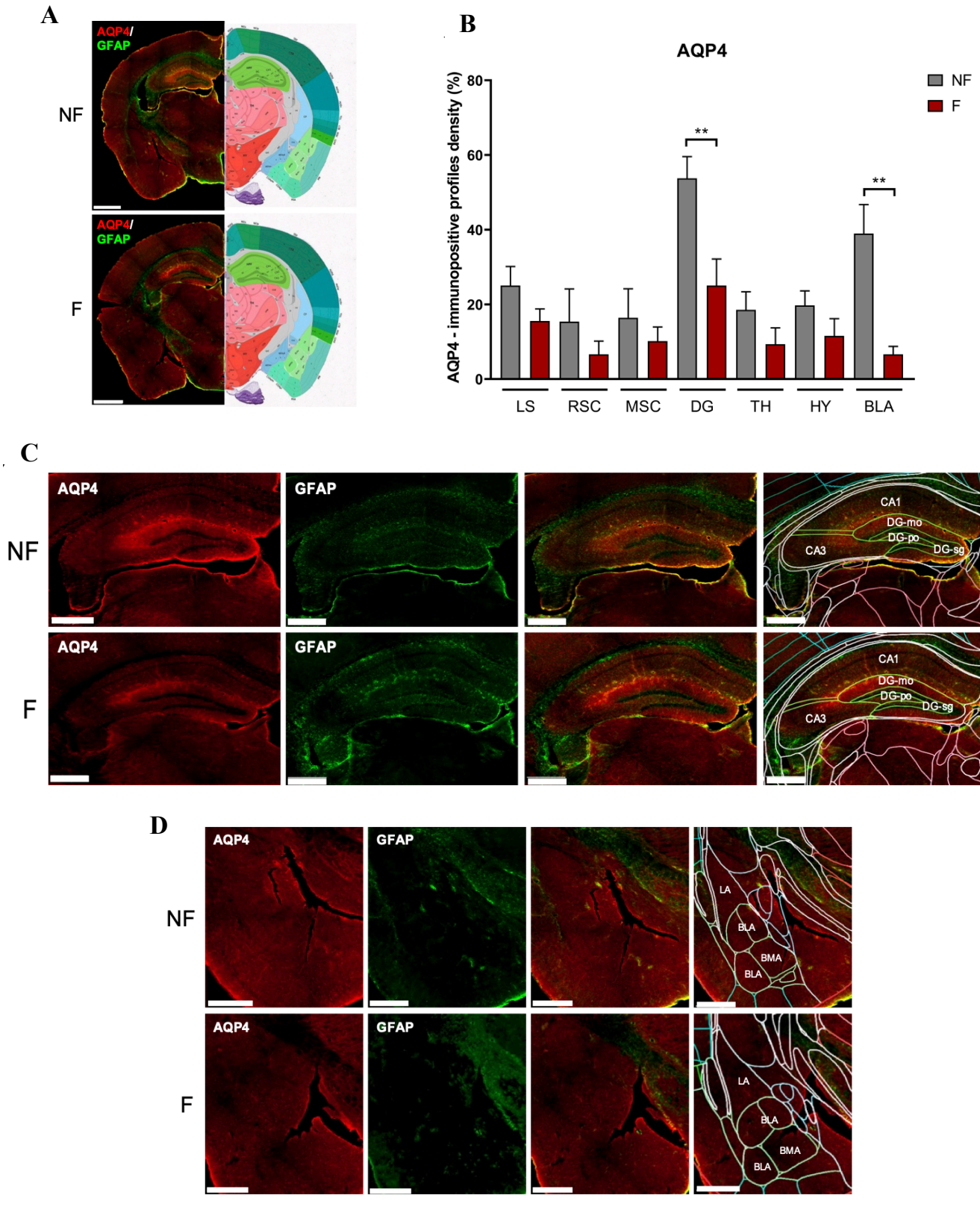

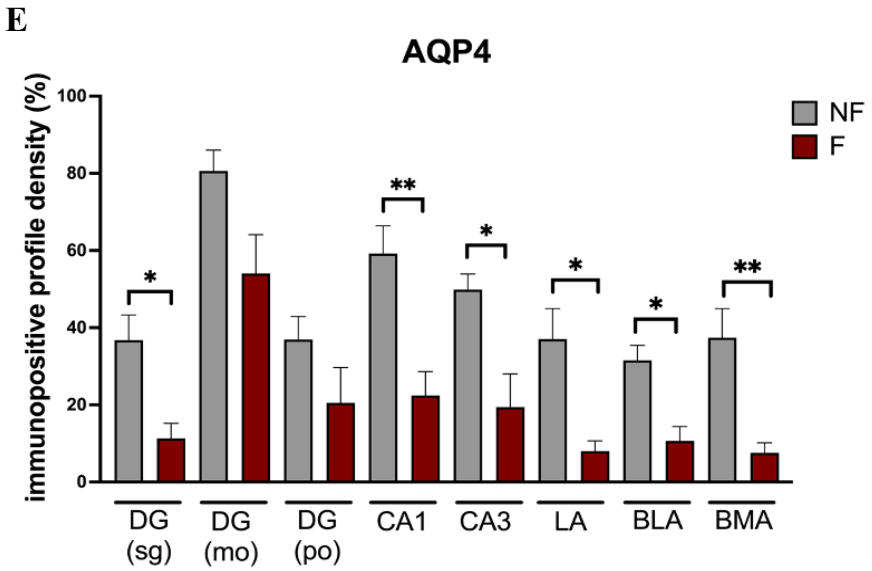

Figure 16. A Representative image of immunohistochemistry of AQP4 antibody. Scale bar 1000 μm. **B** Histogram of AQP4 density. **C** and **D** Representative image of immunohistochemistry of AQP4 and GFAP antibody in the different subregions of hippocampus and amygdala respectively. Scale bar 500 μm. **E** Histogram of AQP4 density. NF=not fragmented mice; F=fragmented mice. LS=lateral septum; RSC=retrosplenial cortex; MSC=motor-sensory cortex; DG=dentate gyrus; TH=thalamus; HY=hypothalamus; BLA=basolateral amygdala; DG (sg)=granule cell layer of the dentate gyrus; DG (mo)=molecular layer of the dentate gyrus; DG (po)=polyphorm layer of the dentate gyrus; LA=lateral amygdala; BMA=basomedial amygdala. The data are mean standard error of the mean (SEM). *p<0,05; **p<0,01; ***p<0,005 versus control by t-test analysis, n=4 per condition.

SF-mediated AQP4 reduction correlates with neuronal activity impairment

As shown in Fig. 17, neuronal activity is reduced in both hippocampus and amygdala after SF. In particular, c-Fos+ nuclei decreased in the CA1 and CA3 hippocampal subregions (Fig. 17A, B) and in the three amygdalar nuclei (LA, BLA, and BMA) (Fig. 17C, D). This data correlates with AQP4 decrease observed in Fig. 16.

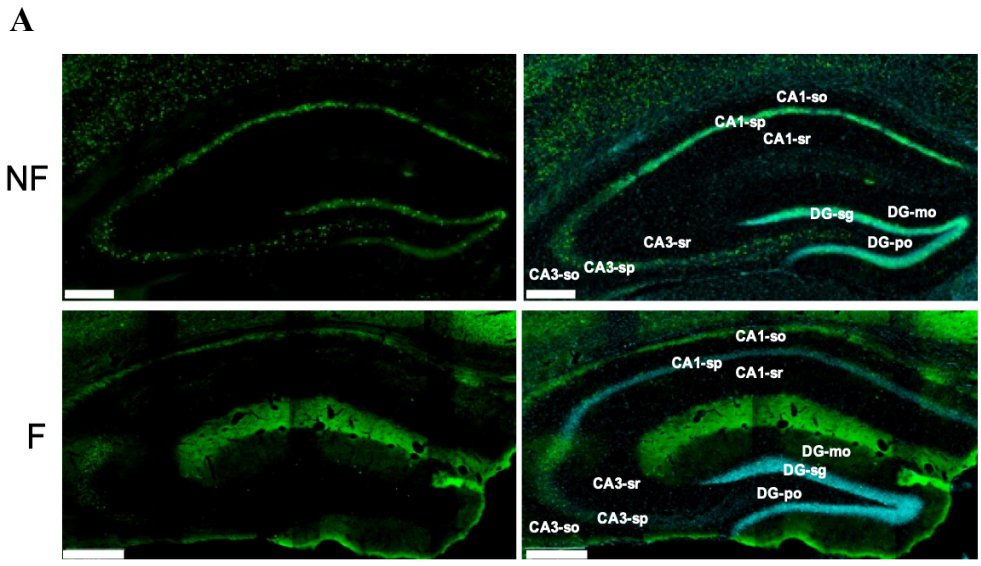

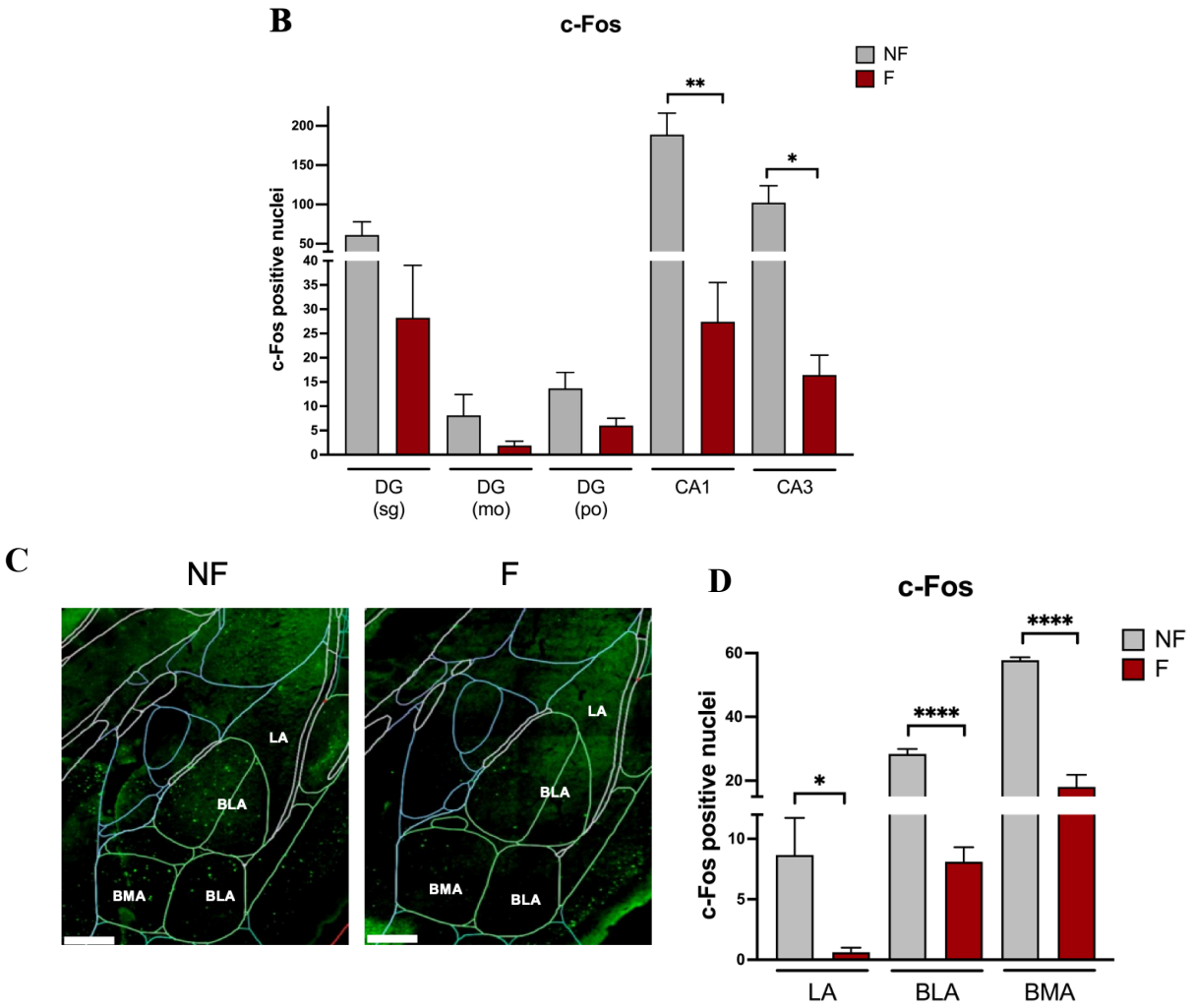

Figure 17. A Representative image of immunohistochemistry of c-Fos antibody in the hippocampus. Scale bar 250 μm. **B** Histogram of c-Fos positive nuclei in the hippocampus. **C** Representative image of immunohistochemistry of c-Fos antibody in the amygdala. Scale bar 250 μm. **D** Histogram of c-Fos positive nuclei in the amygdala. NF=not fragmented mice; F=fragmented mice. DG (sg)=granule cell layer of the dentate gyrus; DG (mo)=molecular layer of the dentate gyrus; DG (po)=polyphorm layer of the dentate gyrus; LA=lateral amygdala; BLA=basolateral amygdala; BMA=basomedial amygdala. The data are mean standard error of the mean (SEM). *p<0,05; **p<0,01; ****p<0,0001 versus control by t-test analysis, n=4 per condition.

Discussion

Sleep plays a pivotal role in neural restoration and the maintenance of various physiological systems[64]. It is a universally conserved phenomenon among mammals, contributing significantly to multiple physiological functions, including cognitive abilities, immune responses, and hormone regulation[132,133]. A typical night sleep in humans consists of alternating periods of NREM and REM sleep, occurring in 5–6 cycles. With aging, sleep patterns naturally change, leading to increased SF, nighttime awakenings, and a greater tendency for daytime sleep[67]. Importantly, disrupted sleep has been linked to cognitive disorders[134]. Indeed, in many psychiatric disorders sleep pattern is not as physiological, but it seems more fragmented. This type of disruption is also common in several kind of sleep diseases, such as insomnia, restless leg syndrome (RLS), periodic limb movement disorder (PLMD), and obstructive sleep apnea syndrome (OSAS)[74,75]. Interestingly, both psychiatric and sleep disorders are considered as risk factors for neurodegenerative diseases like AD. In particular, it is increasingly common to talk about a bidirectional relationship between sleep disorders and AD. In fact, early observations of institutionalized AD patients reveal compromised nocturnal sleep, which is even more pronounced in individuals with mild cognitive impairment (MCI)[53].

SF refers to the disruption of sleep quality caused by frequent disturbances, either from external (e.g., noises) or internal factors (e.g., apnea and limb movements). It involves brief and frequent awakenings followed by a return to sleep, thus impacting the architecture of sleep patterns[73,135,136]. In this study, our analysis of hypnograms under normal conditions and during SF periods confirmed the effectiveness of our experimental protocol. We observed a notable increase in sleep-wake transitions and a decrease in NREM sleep compared to wakefulness in mice exposed to chronic SF. This pattern mimics the sleep disruptions typically seen in aging, AD, and sleep disorders.

Since our aim was to identify SF as a potential risk factor for AD onset and as a target for therapeutic intervention in AD patients to slowdown the disease, we firstly investigated whether SF may contribute to AD pathology. To assess this, we observed the effects of SF in 5xFAD mice considering two different ages: very young (2-month-old) and young adult mice (6-month-old). These animals represent a severe model of AD, characterized by early parenchymal plaque accumulation at just 2 months of age[137]. We demonstrated that SF accelerates AD progression. In particular, in younger mice, we observed a significant increase in Aβ accumulation in regions associated with AD pathology and sleep regulation, contrary to control mice (not fragmented 5xFAD animals). Notably, Aβ accumulation also increased in the lateral septum, a basal forebrain structure linked to anxiety modulation through its connection with the hippocampus[138,139]. This finding aligns with our observations of increased anxiety and hyperactivity in fragmented mice, as

confirmed in behavioral tests. The lateral septum also integrates neuronal inputs from the hippocampus to transform cognitive mapping into actions[140]. Furthermore, another region involved in spatial memory through its neural connections with the hippocampus is the retrosplenial cortex[141]. Both brain regions were highly affected by SF-dependent Aβ accumulation in our experimental protocol.
Notably, we also detected tau phosphorylation in the dentate gyrus of fragmented mice, while this is not evident in the control group. All these data confirmed our observations in which spatial memory is compromised after SF during the Y-maze test.

Sleep plays a vital role in recovering and preparing for the upcoming day. A crucial mechanism that supports this cognitive function is the activity of the glymphatic system[142] . When we sleep, our brain effectively cleans up waste materials generated by neurons throughout the day. This clearing process specifically occurs during deep sleep, the slow wave sleep, which is an important stage of the NREM sleep [54–56]. However, if our sleep is fragmented due to factors like apneas, noise disturbances, or insomnia, we may struggle to reach deep sleep[73]. Consequently, our brain loses its ability to efficiently clear away waste materials, which can accumulate and trigger neuroinflammation, activating all the mechanisms responsible for neurodegeneration. The glymphatic system relies on the perivascular space (PVS), distinct from the interstitial space, to facilitate waste removal. PVS surrounds the cerebral vascular system and is lined by astrocyte end-feet, pericytes, and endothelial cells that form the blood-brain barrier[143,144]. The primary regulator of glymphatic fluid transport is AQP4 channel, mainly expressed in the astrocytic end-feet facing PVS[42]. Mis-localization of AQP4 has been linked to glymphatic malfunction[46,145]. Previous studies have shown that soluble Aβ and tau oligomers are transported out of the brain via AQP4 channels[146]. For those reasons, we aimed to explore whether the increased production of Aβ observed in fragmented 5xFAD mice may be associated with glymphatic system failure. In young fragmented animals, we observed a significant enhance in AQP4 levels. This increase did not appear to be related to channel activity, as it coincided with higher Aβ accumulation. Additionally, AQP4 distribution remained consistent with perivascular areas in fragmented mice, similar to controls. Moreover, AQP4 still colocalized with GFAP+ cells, thus indicating that the increased AQP4 signal is determined by the expression level rather than its release in CSF, which is a typical sign of glymphatic failure[135,136]. This result is subjected to debate, but an additional noteworthy aspect that might elucidate the abnormal rise in AQP4 expression is associated with chronic pathological changes, such as astrogliosis. Astrogliosis could potentially impede CSF flow, possibly through PVS. Changes in PVS geometry due to vasoconstriction, vasodilation, or

astrocytic swelling can affect glymphatic fluid movement[147]. In this work, we observed increased astrocytic activation in fragmented mice, indicating potential astrogliosis, which however is a prevalent characteristic of neuropathological conditions[148,149]. The activation of astrocytes may result from cytokines released by microglia, which are involved in the pathological APP processing pathway[150,151]. We also confirmed astrogliosis through the analysis of microglial morphological complexity.

Interestingly, this increase in AQP4 levels is not evident when the pathology worsens: in older mice SF reduced AQP4 signal, with additional consequences for Aβ clearance. However, this change in AQP4 levels is likely linked to disease progression, as older mice had a higher Aβ burden. This confirms that at a higher Aβ concentration, AQP4 decreases and this event may be due to astrocyte atrophy[152]. However, we did not observe a significant decrease in GFAP signal in older mice, but this may be explained by a further analysis of astrocyte morphology.

We included wt mice to evaluate the consequences of chronic SF in animals without a genetic predisposition to the disease. We investigated whether the glymphatic system may be altered also in this model. Indeed, we firstly noticed a specific reduction of AQP4 levels in the dentate gyrus and the amygdala. The amygdala and the hippocampus are strictly interconnected: the basolateral amygdala (BLA) innervate the *stratum radiatum* and *stratum oriens* of CA1 and CA3, while the basomedial amygdala (BMA) projects to the *stratum lacunosum moleculare* of CA1[129]. We focused our attention on these two brain areas and we recognized that AQP4 reduction was subregion specific. In fact, AQP4 levels decreased in the granule cell layer (sg) of the dentate gyrus (DG), CA1 and CA3 subregions, and in all the three amygdalar nuclei (LA, BLA, BMA). Intriguingly, we observed that this AQP4 reduction mediated by SF correlated with neuronal activity. Indeed, c-Fos+ nuclei decreased in the CA1 and CA3 hippocampal subregions and in the three amygdalar nuclei examined. Those brain regions are involved in memory consolidation, emotion formation and elaboration, and anxiety-like behaviors[129,153]. In particular, BMA inhibition results in a more anxiety-like behavior [154,155]. In fact, in our experimental model, SF resulted in anxiety, stress, and hyperactivity behaviors observed in the three different behavioral tests: EPM, OF, and LD transition tests. This underlines the association between sleep disorders and psychiatric diseases[156]. Notably, we observed that this behavior affected declarative memory, in which the hippocampus and the amygdala are the mainly two regions involved[157]. In fact, as observed in the NOR test, fragmented animals did not recognize and discriminate the novel object, because their total interaction with both objects is significantly reduced compared with controls. Actually, this event may be explained with the increased anxiety and stress due to SF.

Memory consolidation occurs mainly during NREM sleep, which is the most affected sleep stage in our experimental protocol and generally in pathological SF[153]. We decided to investigate the consolidation of different types of memory in which the hippocampus and the amygdala are mainly involved: procedural, spatial, and emotional memories[153]. Indeed, during the puzzle box test, working memory was compromised in fragmented animals, which struggled in remembering where to dig to reach the dark and therefore safer area compared with controls. In addition, in fragmented mice the consolidation of spatial memory was impaired too, as observed in the radial maze test. In fact, fragmented animals took longer to reach the arm in which the stimulus was presented the day before during the training sessions. Notably, not only does the consolidation of procedural memory appear to be compromised by SF, but also the consolidation of emotional memory. Indeed, in the three-chamber test, fragmented animals approached less with the new animal and interacted more with the old one compared with controls. Moreover, in the passive avoidance test, not fragmented mice never even attempted to enter the danger zone in the days following the training, unlike during the learning session (1 hour after the training session). In contrast, fragmented animals repeatedly attempted to enter the danger zone. Interestingly, LA region is involved in fear conditioning memory, in which GABAergic interneurons modulate neural firing and may gate fear conditioning and memory consolidation [158–160]. Thus, it remains to understand which types of neurons are most affected by SF, inhibitory or excitatory neurons. Notably, we mainly evaluated the dorsal hippocampus, while the ventral one is responsible for affective and motivated behaviors and social memory[161,162]. Moreover, ventral CA1 projects to the medial prefrontal cortex, nucleus accumbens, and the amygdala[162]. These connections occur during the sharp wave and ripples, which are specific waves recordable through EEG involved in memory consolidation. These particular waves take place during the NREM sleep, in which different regions exchange information in order to strengthen and consolidate memory[153].

Thus, we can further investigate which are the most affected synaptic connections in SF and how we can relate this altered neuronal activity to AQP4 reduction.

Conclusions

In this study, we offer a new perspective on AQP4 role as a potential key marker in the exploration of sleep disorders as risk factors for neurodegeneration and AD pathogenesis. We developed a new model of SF in which AQP4 appears to lose its functionality, as evidenced by an increased presence of Aβ plaques. This phenomenon is not observed in older mice, where the disease is advanced, and AQP4 levels decreased. This suggests a direct relationship between AD and SF and their impact on the glymphatic system.

The results obtained from young wt animals open up intriguing opportunities for further investigation. Indeed, a better insight in the impact of sleep on young adult and adolescence cognition is essential since the crucial role this developmental stage plays in learning and memory. Furthermore, we can think to AQP4 as a predictive biomarker for the onset of AD, even in middle age, potentially enabling earlier diagnoses. This is of significant importance, given the pressing need to identify early biomarkers that can recognize individuals at higher risk of developing AD.

References

1. *World Alzheimer Report 2023 Reducing dementia risk: never too early, never too late*.
2. Brenowitz WD. Mixed neuropathologies and estimated rates of clinical progression in a large autopsy sample.
3. Mendez, M. F. Early-Onset Alzheimer Disease. *Neurologic Clinics* vol. 35 Preprint at https://doi.org/10.1016/j.ncl.2017.01.005 (2017).
4. Fania, A. *et al.* A Dementia mortality rates dataset in Italy (2012–2019). *Sci Data* **10**, (2023).
5. Stelzmann, R. A., Norman Schnitzlein, H. & Reed Murtagh, F. An english translation of alzheimer's 1907 paper, "über eine eigenartige erkankung der hirnrinde". *Clinical Anatomy* **8**, (1995).
6. Jack, C. R. *et al.* Prediction of AD with MRI-based hippocampal volume in mild cognitive impairment. *Neurology* **52**, (1999).
7. Montine, T. J. *et al.* National institute on aging-Alzheimer's association guidelines for the neuropathologic assessment of Alzheimer's disease: A practical approach. *Acta Neuropathol* **123**, (2012).
8. Glenner, G. G. & Wong, C. W. Alzheimer's disease: Initial report of the purification and characterization of a novel cerebrovascular amyloid protein. *Biochem Biophys Res Commun* **120**, (1984).
9. Lemere, C. A. *et al.* Sequence of deposition of heterogeneous amyloid β-peptides and APO E in down syndrome: Implications for initial events in amyloid plaque formation. *Neurobiol Dis* **3**, (1996).
10. Scheuner, D. *et al.* Secreted amyloid β-protein similar to that in the senile plaques of Alzheimer's disease is increased in vivo by the presenilin 1 and 2 and APP mutations linked to familial Alzheimer's disease. *Nat Med* **2**, (1996).
11. Giliberto, L. *et al.* Mutant presenilin 1 increases the expression and activity of BACE1. *Journal of Biological Chemistry* **284**, (2009).
12. Holsinger, R. M. D., Lee, J. S., Boyd, A., Masters, C. L. & Collins, S. J. CSF BACE1 activity is increased in CJD and Alzheimer disease other dementias. *Neurology* **67**, (2006).
13. Brion, J. P., Couck, A. M., Passareiro, E. & Flament-Durand, J. Neurofibrillary tangles of Alzheimer's disease: An immunohistochemical study. *J Submicrosc Cytol* **17**, (1985).
14. Grundke-Iqbal, I. *et al.* Abnormal phosphorylation of the microtubule-associated protein tau (tau) in Alzheimer cytoskeletal pathology. *Proc Natl Acad Sci U S A* **83**, (1986).
15. Lee, G., Cowan, N. & Kirschner, M. The primary structure and heterogeneity of tau protein from mouse brain. *Science* **239**, 285–288 (1988).

16. Buée, L., Bussière, T., Buée-Scherrer, V., Delacourte, A. & Hof, P. R. Tau protein isoforms, phosphorylation and role in neurodegenerative disorders. *Brain Research Reviews* vol. 33 Preprint at https://doi.org/10.1016/S0165-0173(00)00019-9 (2000).
17. Murray, M. E. *et al.* Clinicopathologic assessment and imaging of tauopathies in neurodegenerative dementias. *Alzheimer's Research and Therapy* vol. 6 Preprint at https://doi.org/10.1186/alzrt231 (2014).
18. Glass, C. K., Saijo, K., Winner, B., Marchetto, M. C. & Gage, F. H. Mechanisms Underlying Inflammation in Neurodegeneration. *Cell* vol. 140 918–934 Preprint at https://doi.org/10.1016/j.cell.2010.02.016 (2010).
19. Block, M. L. & Hong, J. S. Microglia and inflammation-mediated neurodegeneration: Multiple triggers with a common mechanism. *Progress in Neurobiology* vol. 76 77–98 Preprint at https://doi.org/10.1016/j.pneurobio.2005.06.004 (2005).
20. Nimmerjahn, A., Kirchhoff, F. & Helmchen, F. Neuroscience: Resting microglial cells are highly dynamic surveillants of brain parenchyma in vivo. *Science (1979)* **308**, (2005).
21. Streit, W. J., Mrak, R. E. & Griffin, W. S. T. Microglia and neuroinflammation: A pathological perspective. *J Neuroinflammation* **1**, (2004).
22. Zhang, B. *et al.* Targeting MAPK pathways by naringenin modulates microglia M1/M2 polarization in lipopolysaccharide-stimulated cultures. *Front Cell Neurosci* **12**, (2019).
23. Frank-Cannon, T. C., Alto, L. T., McAlpine, F. E. & Tansey, M. G. Does neuroinflammation fan the flame in neurodegenerative diseases? *Mol Neurodegener* **4**, (2009).
24. Jha, M. K., Lee, W. H. & Suk, K. Functional polarization of neuroglia: Implications in neuroinflammation and neurological disorders. *Biochemical Pharmacology* vol. 103 Preprint at https://doi.org/10.1016/j.bcp.2015.11.003 (2016).
25. Tang, Y. & Le, W. Differential Roles of M1 and M2 Microglia in Neurodegenerative Diseases. *Molecular Neurobiology* vol. 53 Preprint at https://doi.org/10.1007/s12035-014-9070-5 (2016).
26. Heneka, M. T. Inflammasome activation and innate immunity in Alzheimer's disease. *Brain Pathology* **27**, (2017).
27. Mandrekar-Colucci, S. & Landreth, G. E. Microglia and Inflammation in Alzheimers Disease. *CNS Neurol Disord Drug Targets* **9**, (2012).
28. Keren-Shaul, H. *et al.* A Unique Microglia Type Associated with Restricting Development of Alzheimer's Disease. *Cell* **169**, (2017).

29. Wolf, S. A., Boddeke, H. W. G. M. & Kettenmann, H. Microglia in Physiology and Disease. *Annual Review of Physiology* vol. 79 Preprint at https://doi.org/10.1146/annurev-physiol-022516-034406 (2017).
30. Jin, J. J., Kim, H. D., Maxwell, J. A., Li, L. & Fukuchi, K. I. Toll-like receptor 4-dependent upregulation of cytokines in a transgenic mouse model of Alzheimer's disease. *J Neuroinflammation* **5**, (2008).
31. Tahara, K. *et al.* Role of toll-like receptor signalling in Aβ uptake and clearance. *Brain* **129**, (2006).
32. Mucke, L. & Eddleston, M. Astrocytes in infectious and immune-mediated diseases of the central nervous system. *The FASEB Journal* **7**, (1993).
33. Kato, S. *et al.* Confocal observation of senile plaques in Alzheimer's disease: Senile plaque morphology and relationship between senile plaques and astrocytes. *Pathol Int* **48**, (1998).
34. Wegiel, J. *et al.* The role of microglial cells and astrocytes in fibrillar plaque evolution in transgenic APPSW mice. *Neurobiol Aging* **22**, (2001).
35. Kraft, A. W. *et al.* Attenuating astrocyte activation accelerates plaque pathogenesis in APP/PS1 mice. *FASEB Journal* **27**, (2013).
36. Wyss-Coray, T. *et al.* Adult mouse astrocytes degrade amyloid-β in vitro and in situ. *Nat Med* **9**, (2003).
37. Paudel, Y. N. *et al.* Impact of HMGB1, RAGE, and TLR4 in Alzheimer's Disease (AD): From Risk Factors to Therapeutic Targeting. *Cells* vol. 9 Preprint at https://doi.org/10.3390/cells9020383 (2020).
38. Lim, G. P. *et al.* The curry spice curcumin reduces oxidative damage and amyloid pathology in an Alzheimer transgenic mouse. *Journal of Neuroscience* **21**, (2001).
39. Hoppe, J. B., Haag, M., Whalley, B. J., Salbego, C. G. & Cimarosti, H. Curcumin protects organotypic hippocampal slice cultures from Aβ1-42-induced synaptic toxicity. *Toxicology in Vitro* **27**, (2013).
40. Khan, H., Ullah, H., Aschner, M., Cheang, W. S. & Akkol, E. K. Neuroprotective effects of quercetin in alzheimer's disease. *Biomolecules* vol. 10 Preprint at https://doi.org/10.3390/biom10010059 (2020).
41. Moussa, C. *et al.* Resveratrol regulates neuro-inflammation and induces adaptive immunity in Alzheimer's disease. *J Neuroinflammation* **14**, (2017).
42. Iliff, J. J. *et al.* A Paravascular Pathway Facilitates CSF Flow Through the Brain Parenchyma and the Clearance of Interstitial Solutes, Including Amyloid β. *Sci Transl Med* **4**, (2012).

43. Xie, L. *et al.* Sleep drives metabolite clearance from the adult brain. *Science (1979)* **342**, (2013).
44. Rainey-Smith, S. R. *et al.* Genetic variation in Aquaporin-4 moderates the relationship between sleep and brain Aβ-amyloid burden. *Transl Psychiatry* **8**, (2018).
45. Tarasoff-Conway, J. M. *et al.* Clearance systems in the brain—implications for Alzheimer disease. *Nat Rev Neurol* **11**, 457–470 (2015).
46. Mestre, H. *et al.* Aquaporin-4-dependent glymphatic solute transport in the rodent brain. *Elife* **7**, (2018).
47. Smith, A. J., Yao, X., Dix, J. A., Jin, B. J. & Verkman, A. S. Test of the 'glymphatic' hypothesis demonstrates diffusive and aquaporin-4-independent solute transport in rodent brain parenchyma. *Elife* **6**, (2017).
48. Nedergaard, M. & Goldman, S. A. Glymphatic failure as a final common pathway to dementia. *Science (1979)* **370**, (2020).
49. Xu, Z. *et al.* Deletion of aquaporin-4 in APP/PS1 mice exacerbates brain Aβ accumulation and memory deficits. *Mol Neurodegener* **10**, 58 (2015).
50. Lee, H. *et al.* The effect of body posture on brain glymphatic transport. *Journal of Neuroscience* **35**, (2015).
51. Levendowski, D. J. *et al.* Head position during sleep: Potential implications for patients with neurodegenerative disease. *Journal of Alzheimer's Disease* **67**, (2019).
52. Ju, Y. E. S., Lucey, B. P. & Holtzman, D. M. Sleep and Alzheimer disease pathology-a bidirectional relationship. *Nature Reviews Neurology* vol. 10 Preprint at https://doi.org/10.1038/nrneurol.2013.269 (2014).
53. da Silva, R. A. P. C. Sleep disturbances and mild cognitive impairment: A review. *Sleep Science* vol. 8 Preprint at https://doi.org/10.1016/j.slsci.2015.02.001 (2015).
54. Steele, T. A., St Louis, E. K., Videnovic, A. & Auger, R. R. Circadian Rhythm Sleep–Wake Disorders: a Contemporary Review of Neurobiology, Treatment, and Dysregulation in Neurodegenerative Disease. *Neurotherapeutics* vol. 18 Preprint at https://doi.org/10.1007/s13311-021-01031-8 (2021).
55. Schlosser Covell, G. E. *et al.* Disrupted daytime activity and altered sleep-wake patterns may predict transition to mild cognitive impairment or dementia: A critically appraised topic. *Neurologist* **18**, (2012).
56. Lim, A. S. P., Kowgier, M., Yu, L., Buchman, A. S. & Bennett, D. A. Sleep fragmentation and the risk of incident Alzheimer's disease and cognitive decline in older persons. *Sleep* **36**, (2013).

57. Atherton, L. A., Dupret, D. & Mellor, J. R. Memory trace replay: The shaping of memory consolidation by neuromodulation. *Trends in Neurosciences* vol. 38 Preprint at https://doi.org/10.1016/j.tins.2015.07.004 (2015).
58. Nishida, M., Pearsall, J., Buckner, R. L. & Walker, M. P. REM sleep, prefrontal theta, and the consolidation of human emotional memory. *Cerebral Cortex* **19**, (2009).
59. Sopp, M. R., Michael, T., Weeß, H. G. & Mecklinger, A. Remembering specific features of emotional events across time: The role of REM sleep and prefrontal theta oscillations. *Cogn Affect Behav Neurosci* **17**, (2017).
60. Krueger, J., Walter, J. & Levin, C. Factor S and Related Somnogens: An Immune Theory for Slow-Wave Sleep. Appendix I,. *Brain mechanisms of sleep* **7**, (1985).
61. Toth, L. A., Tolley, E. A. & Krueger, J. M. Sleep as a Prognostic Indicator During Infectious Disease in Rabbits. *Proceedings of the Society for Experimental Biology and Medicine* **203**, (1993).
62. Mang, G. M. & Franken, P. Sleep and EEG Phenotyping in Mice. in *Current Protocols in Mouse Biology* (2012). doi:10.1002/9780470942390.mo110126.
63. Colten, H. R. & Altevogt, B. M. *Sleep disorders and sleep deprivation: An unmet public health problem*. *Sleep Disorders and Sleep Deprivation: An Unmet Public Health Problem* (2006). doi:10.17226/11617.
64. Siegel, J. M. Clues to the functions of mammalian sleep. *Nature* **437**, (2005).
65. Kryger, M. H., Dement, W. C. & Roth, T. *Principles and practice of sleep medicine*. *Principles and Practice of Sleep Medicine, 5th Edition* (2010). doi:10.1016/C2009-0-59875-3.
66. Stickgold, R. Sleep: Off-line memory reprocessing. *Trends in Cognitive Sciences* vol. 2 Preprint at https://doi.org/10.1016/S1364-6613(98)01258-3 (1998).
67. Ohayon, M. M., Carskadon, M. A., Guilleminault, C. & Vitiello, M. V. Meta-analysis of quantitative sleep parameters from childhood to old age in healthy individuals: Developing normative sleep values across the human lifespan. *Sleep* **27**, (2004).
68. Van Gool, W. A. & Mirmiran, M. Age-related changes in the sleep pattern of male adult rats. *Brain Res* **279**, (1983).
69. Shiromani, P. J. *et al.* Compensatory sleep response to 12 h wakefulness in young and old rats. *Am J Physiol Regul Integr Comp Physiol* **278**, (2000).
70. Welsh, D. K., Richardson, G. S. & Dement, W. C. Effect of age on the circadian pattern of sleep and wakefulness in the mouse. *Journals of Gerontology* **41**, (1986).

71. Eleftheriou, B. E., Zolovick, A. J. & Elias, M. F. Electroencephalographic changes with age in male mice. *Gerontology* **21**, (1975).
72. Vitaterna, M. H., Takahashi, J. S. & Turek, F. W. Overview of circadian rhythms. *Alcohol Research and Health* **25**, (2001).
73. Stepanski, E., Lamphere, J., Badia, P., Zorick, F. & Roth, T. Sleep fragmentation and daytime sleepiness. *Sleep* **7**, (1984).
74. Roehrs, T. *et al.* Sleep-wake complaints in patients with sleep-related respiratory disturbances. *American Review of Respiratory Disease* **132**, (1985).
75. Saletu, M. *et al.* Sleep Laboratory Studies in Restless Legs Syndrome Patients as Compared with Normals and Acute Effects of Ropinirole. *Neuropsychobiology* **41**, (2000).
76. Riemann, D., Krone, L. B., Wulff, K. & Nissen, C. Sleep, insomnia, and depression. *Neuropsychopharmacology* vol. 45 Preprint at https://doi.org/10.1038/s41386-019-0411-y (2020).
77. Pigeon, W. R., Pinquart, M. & Conner, K. Meta-analysis of sleep disturbance and suicidal thoughts and behaviors. *Journal of Clinical Psychiatry* vol. 73 Preprint at https://doi.org/10.4088/JCP.11r07586 (2012).
78. Li, M., Zhang, X. W., Hou, W. S. & Tang, Z. Y. Insomnia and risk of cardiovascular disease: A meta-analysis of cohort studies. *Int J Cardiol* **176**, (2014).
79. Sahlin, C. *et al.* Obstructive sleep apnea is a risk factor for death in patients with stroke: A 10-year follow-up. *Arch Intern Med* **168**, (2008).
80. Hermann, D. M. & Bassetti, C. L. Role of sleep-disordered breathing and sleep-wake disturbances for stroke and stroke recovery. *Neurology* vol. 87 Preprint at https://doi.org/10.1212/WNL.0000000000003037 (2016).
81. Shi, L. *et al.* Sleep disturbances increase the risk of dementia: A systematic review and meta-analysis. *Sleep Medicine Reviews* vol. 40 Preprint at https://doi.org/10.1016/j.smrv.2017.06.010 (2018).
82. Cooke, J. R. & Ancoli-Israel, S. *Normal and abnormal sleep in the elderly*. *Handbook of Clinical Neurology* vol. 98 (2011).
83. Stickgold, R. Sleep-dependent memory consolidation. *Nature* vol. 437 Preprint at https://doi.org/10.1038/nature04286 (2005).
84. Plihal, W. & Born, J. Effects of early and late nocturnal sleep on declarative and procedural memory. *J Cogn Neurosci* **9**, (1997).
85. Gais, S. & Born, J. Declarative memory consolidation: Mechanisms acting during human sleep. *Learning and Memory* vol. 11 Preprint at https://doi.org/10.1101/lm.80504 (2004).

86. Diba, K. & Buzsáki, G. Forward and reverse hippocampal place-cell sequences during ripples. *Nat Neurosci* **10**, (2007).
87. Steriade, M., Nunez, A. & Amzica, F. A novel slow (< 1 Hz) oscillation of neocortical neurons in vivo: Depolarizing and hyperpolarizing components. *Journal of Neuroscience* **13**, (1993).
88. Steriade, M. Grouping of brain rhythms in corticothalamic systems. *Neuroscience* vol. 137 Preprint at https://doi.org/10.1016/j.neuroscience.2005.10.029 (2006).
89. Steriade, M., Deschenes, M., Domich, L. & Mulle, C. Abolition of spindle oscillations in thalamic neurons disconnected from nucleus reticularis thalami. *J Neurophysiol* **54**, (1985).
90. Staresina, B. P. *et al.* Hierarchical nesting of slow oscillations, spindles and ripples in the human hippocampus during sleep. *Nat Neurosci* **18**, (2015).
91. Sirota, A., Csicsvari, J., Buhl, D. & Buzsáki, G. Communication between neocortex and hippocampus during sleep in rodents. *Proc Natl Acad Sci U S A* **100**, (2003).
92. Rothschild, G., Eban, E. & Frank, L. M. A cortical-hippocampal-cortical loop of information processing during memory consolidation. *Nat Neurosci* **20**, (2017).
93. Van Gool, W. A. & Mirmiran, M. Effects of aging and housing in an enriched environment on sleep-wake patterns in rats. *Sleep* **9**, (1986).
94. Gutwein, B. M. & Fishbein, W. Paradoxical sleep and memory (II): Sleep circadian rhythmicity following enriched and impoverished environmental rearing. *Brain Res Bull* **5**, (1980).
95. Born, J. & Gais, S. REM sleep deprivation: The wrong paradigm leading to wrong conclusions. *Behavioral and Brain Sciences* **23**, (2000).
96. Poe, G. R., Walsh, C. M. & Bjorness, T. E. Cognitive neuroscience of sleep. in *Progress in Brain Research* vol. 185 (2010).
97. MacDonald, K. J. & Cote, K. A. Contributions of post-learning REM and NREM sleep to memory retrieval. *Sleep Medicine Reviews* vol. 59 Preprint at https://doi.org/10.1016/j.smrv.2021.101453 (2021).
98. Li, W., Ma, L., Yang, G. & Gan, W. B. REM sleep selectively prunes and maintains new synapses in development and learning. *Nat Neurosci* **20**, (2017).
99. Zhou, Y. *et al.* REM sleep promotes experience-dependent dendritic spine elimination in the mouse cortex. *Nat Commun* **11**, (2020).
100. Yoo, S. S., Gujar, N., Hu, P., Jolesz, F. A. & Walker, M. P. The human emotional brain without sleep - a prefrontal amygdala disconnect. *Current Biology* vol. 17 Preprint at https://doi.org/10.1016/j.cub.2007.08.007 (2007).

101. Alhola, P. & Polo-Kantola, P. Sleep deprivation: Impact on cognitive performance. *Neuropsychiatric Disease and Treatment* vol. 3 Preprint at (2007).
102. Yoo, S. S., Hu, P. T., Gujar, N., Jolesz, F. A. & Walker, M. P. A deficit in the ability to form new human memories without sleep. *Nat Neurosci* **10**, (2007).
103. Beebe, D. W. *et al.* Feasibility and behavioral effects of an at-home multi-night sleep restriction protocol for adolescents. *J Child Psychol Psychiatry* **49**, (2008).
104. Loessl, B. *et al.* Are adolescents chronically sleep-deprived? An investigation of sleep habits of adolescents in the Southwest of Germany. *Child Care Health Dev* **34**, (2008).
105. Carskadon, M. A. Factors Influencing Sleep Patterns of Adolescents. in *Adolescent Sleep Patterns* (2009). doi:10.1017/cbo9780511499999.005.
106. Crowley, S. J., Acebo, C. & Carskadon, M. A. Sleep, circadian rhythms, and delayed phase in adolescence. *Sleep Med* **8**, (2007).
107. Van Cauter, E., Leproult, R. & Plat, L. Age-related changes in slow wave sleep and REM sleep and relationship with growth hormone and cortisol levels in healthy men. *JAMA* **284**, (2000).
108. Wang, C. & Holtzman, D. M. Bidirectional relationship between sleep and Alzheimer's disease: role of amyloid, tau, and other factors. *Neuropsychopharmacology* vol. 45 Preprint at https://doi.org/10.1038/s41386-019-0478-5 (2020).
109. Lucey, B. P. *et al.* Effect of sleep on overnight cerebrospinal fluid amyloid β kinetics. *Ann Neurol* **83**, (2018).
110. Ooms, S. *et al.* Effect of 1 night of total sleep deprivation on cerebrospinal fluid β-amyloid 42 in healthy middle-aged men a randomized clinical trial. *JAMA Neurol* **71**, (2014).
111. Roh, J. H. *et al.* Disruption of the sleep-wake cycle and diurnal fluctuation of amyloid-β in mice with Alzheimer's disease pathology. *Sci Transl Med* **4**, (2012).
112. Holth, J. K. *et al.* The sleep-wake cycle regulates brain interstitial fluid tau in mice and CSF tau in humans. *Science (1979)* **363**, (2019).
113. McCurry, S. M., Reynolds, C. F., Ancoli-Israel, S., Teri, L. & Vitiello, M. V. Treatment of sleep disturbance in Alzheimer's disease. *Sleep Med Rev* **4**, (2000).
114. Hahn, E. A., Wang, H. X., Andel, R. & Fratiglioni, L. A change in sleep pattern may predict alzheimer disease. *American Journal of Geriatric Psychiatry* **22**, (2014).
115. Bastianini, S. *et al.* SCOPRISM: A new algorithm for automatic sleep scoring in mice. *J Neurosci Methods* **235**, (2014).

116. Carola, V., D'Olimpio, F., Brunamonti, E., Mangia, F. & Renzi, P. Evaluation of the elevated plus-maze and open-field tests for the assessment of anxiety-related behaviour in inbred mice. *Behavioural Brain Research* **134**, (2002).
117. Antunes, M. & Biala, G. The novel object recognition memory: Neurobiology, test procedure, and its modifications. *Cognitive Processing* vol. 13 Preprint at https://doi.org/10.1007/s10339-011-0430-z (2012).
118. Takao, K. & Miyakawa, T. Light/dark transition test for mice. *Journal of Visualized Experiments* (2006) doi:10.3791/104.
119. O'Connor, A. M., Burton, T. J., Leamey, C. A. & Sawatari, A. The use of the puzzle box as a means of assessing the efficacy of environmental enrichment. *Journal of Visualized Experiments* (2014) doi:10.3791/52225.
120. Shoji, H. & Miyakawa, T. Age-related behavioral changes from young to old age in male mice of a C57BL/6J strain maintained under a genetic stability program. *Neuropsychopharmacol Rep* **39**, (2019).
121. Kruk-Slomka, M. & Biala, G. Cannabidiol attenuates mk-801-induced cognitive symptoms of schizophrenia in the passive avoidance test in mice. *Molecules* **26**, (2021).
122. Bolte, S. & Cordelières, F. P. A guided tour into subcellular colocalization analysis in light microscopy. *Journal of Microscopy* vol. 224 Preprint at https://doi.org/10.1111/j.1365-2818.2006.01706.x (2006).
123. Young, K. & Morrison, H. Quantifying microglia morphology from photomicrographs of immunohistochemistry prepared tissue using imagej. *Journal of Visualized Experiments* **2018**, (2018).
124. Davies, D. S., Ma, J., Jegathees, T. & Goldsbury, C. Microglia show altered morphology and reduced arborization in human brain during aging and Alzheimer's disease. *Brain Pathology* **27**, (2017).
125. Bankhead, P. *et al.* QuPath: Open source software for digital pathology image analysis. *Sci Rep* **7**, (2017).
126. Wang, C. *et al.* A comparative study of sleep and diurnal patterns in house mouse (Mus musculus) and Spiny mouse (Acomys cahirinus). *Sci Rep* **10**, (2020).
127. Fritz, E. M., Kreuzer, M., Altunkaya, A., Singewald, N. & Fenzl, T. Altered sleep behavior in a genetic mouse model of impaired fear extinction. *Sci Rep* **11**, (2021).
128. Wimmer, M. E. *et al.* Aging in mice reduces the ability to sustain sleep/wake states. *PLoS One* **8**, (2013).

129. McGaugh, J. L. The amygdala modulates the consolidation of memories of emotionally arousing experiences. *Annual Review of Neuroscience* vol. 27 Preprint at https://doi.org/10.1146/annurev.neuro.27.070203.144157 (2004).
130. Li, Y. K. *et al.* Aquaporin-4 deficiency impairs synaptic plasticity and associative fear memory in the lateral amygdala: Involvement of downregulation of glutamate transporter-1 expression. *Neuropsychopharmacology* **37**, (2012).
131. Skucas, V. A. *et al.* Impairment of select forms of spatial memory and neurotrophin-dependent synaptic plasticity by deletion of glial aquaporin-4. *Journal of Neuroscience* **31**, (2011).
132. Irwin, M. R. Why sleep is important for health: A psychoneuroimmunology perspective. *Annu Rev Psychol* **66**, (2015).
133. Krause, A. J. *et al.* The sleep-deprived human brain. *Nat Rev Neurosci* **18**, (2017).
134. Killgore, W. D. S. Effects of sleep deprivation on cognition. *Prog Brain Res* **185**, 105–129 (2010).
135. Jarius, S. *et al.* Cerebrospinal fluid antibodies to aquaporin-4 in neuromyelitis optica and related disorders: Frequency, origin, and diagnostic relevance. *J Neuroinflammation* **7**, (2010).
136. Papadopoulos, M. C. & Verkman, A. S. Aquaporin-4 and brain edema. *Pediatric Nephrology* vol. 22 Preprint at https://doi.org/10.1007/s00467-006-0411-0 (2007).
137. Oakley, H. *et al.* Intraneuronal β-amyloid aggregates, neurodegeneration, and neuron loss in transgenic mice with five familial Alzheimer's disease mutations: Potential factors in amyloid plaque formation. *Journal of Neuroscience* **26**, (2006).
138. Trent, N. L. & Menard, J. L. The ventral hippocampus and the lateral septum work in tandem to regulate rats' open-arm exploration in the elevated plus-maze. *Physiol Behav* **101**, (2010).
139. Parfitt, G. M. *et al.* Bidirectional Control of Anxiety-Related Behaviors in Mice: Role of Inputs Arising from the Ventral Hippocampus to the Lateral Septum and Medial Prefrontal Cortex. *Neuropsychopharmacology* **42**, (2017).
140. Tingley, D. & Buzsáki, G. Transformation of a Spatial Map across the Hippocampal-Lateral Septal Circuit. *Neuron* **98**, (2018).
141. Balcerek, E., Włodkowska, U. & Czajkowski, R. Retrosplenial cortex in spatial memory: focus on immediate early genes mapping. *Mol Brain* **14**, (2021).
142. Hablitz, L. M. *et al.* Circadian control of brain glymphatic and lymphatic fluid flow. *Nat Commun* **11**, 4411 (2020).

143. Simard, M., Arcuino, G., Takano, T., Liu, Q. S. & Nedergaard, M. Signaling at the gliovascular interface. *Journal of Neuroscience* **23**, (2003).
144. Troili, F. *et al.* Perivascular Unit: This Must Be the Place. The Anatomical Crossroad Between the Immune, Vascular and Nervous System. *Front Neuroanat* **14**, (2020).
145. Wei, F. *et al.* Chronic stress impairs the aquaporin-4-mediated glymphatic transport through glucocorticoid signaling. *Psychopharmacology (Berl)* **236**, (2019).
146. Kress, B. T. *et al.* Impairment of paravascular clearance pathways in the aging brain. *Ann Neurol* **76**, 845–861 (2014).
147. Mestre, H. *et al.* Cerebrospinal fluid influx drives acute ischemic tissue swelling. *Science (1979)* **367**, (2020).
148. Kovacs, G. G., Yousef, A., Kaindl, S., Lee, V. M. & Trojanowski, J. Q. Connexin-43 and aquaporin-4 are markers of ageing-related tau astrogliopathy (ARTAG)-related astroglial response. *Neuropathol Appl Neurobiol* **44**, (2018).
149. Verkhratsky, A., Steardo, L., Parpura, V. & Montana, V. Translational potential of astrocytes in brain disorders. *Prog Neurobiol* **144**, (2016).
150. Liddelow, S. A. *et al.* Neurotoxic reactive astrocytes are induced by activated microglia. *Nature* **541**, 481–487 (2017).
151. Liaoi, Y. F., Wang, B. J., Cheng, H. T., Kuo, L. H. & Wolfe, M. S. Tumor necrosis factor-α, interleukin-1β, and interferon-γ stimulate γ-secretase-mediated cleavage of amyloid precursor protein through a JNK-dependent MAPK pathway. *Journal of Biological Chemistry* **279**, (2004).
152. Yang, W. *et al.* Aquaporin-4 mediates astrocyte response to β-amyloid. *Molecular and Cellular Neuroscience* **49**, 406–414 (2012).
153. Kroeger, D. & Vetrivelan, R. To sleep or not to sleep – Effects on memory in normal aging and disease. *Aging Brain* **3**, 100068 (2023).
154. Amano, T., Duvarci, S., Popa, D. & Paré, D. The fear circuit revisited: Contributions of the basal amygdala nuclei to conditioned fear. *Journal of Neuroscience* **31**, (2011).
155. Adhikari, A. *et al.* Basomedial amygdala mediates top-down control of anxiety and fear. *Nature* **527**, (2015).
156. Sateia, M. J. Update on sleep and psychiatric disorders. *Chest* **135**, (2009).
157. Yang, Y. & Wang, J. Z. From structure to behavior in basolateral amygdala-hippocampus circuits. *Frontiers in Neural Circuits* vol. 11 Preprint at https://doi.org/10.3389/fncir.2017.00086 (2017).

158. Stork, O. & Pape, H. C. Fear memory and the amygdala: Insights from a molecular perspective. *Cell and Tissue Research* vol. 310 Preprint at https://doi.org/10.1007/s00441-002-0656-2 (2002).
159. Szinyei, C., Narayanan, R. T. & Pape, H. C. Plasticity of inhibitory synaptic network interactions in the lateral amygdala upon fear conditioning in mice. *European Journal of Neuroscience* **25**, (2007).
160. Johansen, J. P., Cain, C. K., Ostroff, L. E. & Ledoux, J. E. Molecular mechanisms of fear learning and memory. *Cell* vol. 147 Preprint at https://doi.org/10.1016/j.cell.2011.10.009 (2011).
161. Okuyama, T., Kitamura, T., Roy, D. S., Itohara, S. & Tonegawa, S. Ventral CA1 neurons store social memory. *Science (1979)* **353**, (2016).
162. Ciocchi, S., Passecker, J., Malagon-Vina, H., Mikus, N. & Klausberger, T. Selective information routing by ventral hippocampal CA1 projection neurons. *Science (1979)* **348**, (2015).
163. Wright, K. P. EEG in Sleep States. in *Encyclopedia of Neuroscience* (2008). doi:10.1007/978-3-540-29678-2_2892.